Designing of nanocarriers for therapeutic applications

Maria Inês Martins Lobo de Araújo Correia

Master degree in Quality Control

Dissertation thesis for the Master degree in Quality Control submitted to the Faculty of Pharmacy

Dissertação do 2º Ciclo de Estudos Conducente ao Grau de Mestre em Controlo de Qualidade apresentada à Faculdade de Farmácia

Supervisors:

Dr. Sangram Keshari Samal

Prof. Doctor Kevin Braeckmans

Prof. Doutora Maria de Lourdes Pinho de Almeida Souteiro Bastos

University of Porto

October 2015

Experimental work carried out at the Laboratory of General Biochemistry & Physical Pharmacy,

Faculty of Pharmaceutical Sciences, Ghent University

Acknowledgments

With the end of this thesis I find the need to thank to all the people that contributed to its realization, directly or indirectly.

First of all, I would like to thank to my supervisor Prof. Dra. Maria de Lourdes Bastos for the opportunity to work under her guidance, for all the help when I was still looking for a destination to elaborate this thesis, for all the patience during endless emails exchanged and for all the support when I came back, thank you.

Secondly, I want to thank Dr. Sangram for the daily support, for the scientific and life lessons he taught me and for correcting my thesis.

I am grateful for my promotor in Gent, Prof. Dr. Kevin Braeckmans for the opportunity to participate in the Laboratory of General Biochemistry and Physical Pharmacy and for the valuable experience and guidance.

My sincere thanks also goes to all my colleagues in the lab, specially to Eline and Lotte, for being there for me, supporting me and teaching me everything they could. Thank you for your smiles, it wouldn't have been possible without you. Thank you Cristiana, Diana and Rita for all the comforting moments of hearing our mother tongue spoken in the lab.

To all my friends, the ones I've known forever and the ones I knew in Gent, thank you for the moments of laughter, for believing and always being there for me! BEST Porto, Coleguinhas de Biologia e do MCQ, Miguxas and Seixos, you wil be in my heart forever.

I want to specially thank António, for always believing in me, for making me the better version of myself and for all the support given millions of kilometers away.

The biggest thank you goes to my family, specially my parents and brother, without whom I couldn't ever dream to accomplish this and to have such an amazing adventure studying abroad. Thank you from the bottom of my heart.

Abstract

Nanotechnology is a developing area in science and technology that is being widely explored during the last decade and is one of the most important areas related to drug delivery, cancer treatment and diagnosis. The development of nanocarriers that can offer multiple advantages and a wide range of solutions for drug delivery and imaging properties is interesting and provides challenges and great benefits if well accomplished. Therefore, the aim of this study was to design a nanocarrier capable of transporting a therapeutic agent while providing imaging information regarding the environment of the cancer site.

PLGA nanoparticles and AuNPs were developed with the aim to form a multiple functional nanoparticle, capable of therapeutic effect by transferring light triggered to heat, offering targeted treatment. The nanoparticles were developed and their cytotoxicity, transfection and microscopy assays were performed, in order to evaluate the nanoparticles' characteristics and their therapeutic potential.

Monodispersed AuNPs synthesized at room temperature by simultaneously using two reducing agents (Sodium citrate and Sodium borohydride), showed to be more stable and reproducible when compared to those prepared by the conventional method. The adopted preparation technique of the organic biodegradable PLGA NPs offers better control over size, polydispersity index and surface charge, allowing modification of its surface with the cationic polymers chitosan or protamine and incorporation of QDs. The cytotoxicity analysis of the prepared nanocarriers showed no remarkable toxic effects to HeLa cells in the conditions of the assay. The cationic PLGA NPs showed good nucleic acid complexation ability although did not show good transfection potential.

The utilization of the prepared nanocarriers has to be investigated further in detail.

Keywords: gold nanoparticles, PLGA nanoparticles, Quantum dots, nanocarriers, cytotoxicity, transfection, complexation, pDNA, siRNA, SPT, FCS

Resumo

A Nanotecnologia é uma área da ciência e tecnologia em franco desenvolvimento, tendo-se assistido na última década a uma expansão impressionante do seu âmbito de aplicação. Nomeadamente no âmbito da oncologia, é considerada uma das mais importantes áreas relacionadas com a libertação de fármacos e com o tratamento e diagnóstico do cancro. O desenvolvimento de nanotransportadores pode oferecer múltiplas vantagens e soluções para esta temática, potencialmente muito interessantes e desafiantes, trazendo grandes benefícios em caso de sucesso.

Assim sendo, o objectivo deste estudo foi desenhar um nanotransportador capaz de libertar um agente terapêutico e ao mesmo tempo fornecer informação relativa ao ambiente circundante da localização do cancro.

Nanopartículas de PLGA e de ouro foram desenvolvidas com o objectivo de criar uma nanopartícula multifuncional, capaz de produzir efeitos terapêuticos ao ser activada por luz pulsada em locais alvo. As nanopartículas foram desenvolvidas e a sua citotoxicidade e eficiência de transfecção foram testadas, bem como realizados ensaios de microscopia, para avaliar as características das mesmas e o seu potencial terapêutico.

Nanopartículas de ouro monodispersas foram sintetizadas à temperatura ambiente, utilizando simultaneamente dois agentes reductores (citrato de sódio e boro-hidreto de sódio) que demonstraram ser o método mais estável e reprodutível de preparação das nanopartículas, em comparação com o método tradicional. A técnica de preparação adoptada para a formação de nanopartículas orgânicas e biodegradáveis de PLGA, oferece um melhor controlo relativamente ao seu tamanho, índice de polidispersão e carga da superfície, permitindo a modificação da sua superfície exterior com os polímeros catiónicos quitosana ou protamina e ainda a incorporação de QDs. A análise citotóxica efectuada dos nanotransportadores preparados não demonstrou efeitos tóxicos significativos nas células HeLa nas condições testadas. As nanopartículas de PLGA catiónicas mostraram uma boa capacidade de complexação de ácidos nucleicos, no entanto, não mostraram uma boa eficiência de transfecção.

A utilização das nanopartículas preparadas deve ser investigada em detalhe.

Palavras-chave: nanopartículas de ouro, nanopartículas de PLGA, Quantum dots, nanotransportadores, citotoxicidade, transfecção, complexação, pDNA, siRNA, SPT, FCS

Table of Contents

List of Figures

List of Tables

Abbreviations and symbols

µL-	microliter
µM-	micromolar
Au-	bulk gold
AuNPs-	gold nanoparticles
bPEI-	branched Polyethylenimine
BSA-	bovine serum albumin
CCM-	cell culture medium
cDNA-	complementary DNA
CO_2-	carbon dioxide
CT-	computer tomography
CTAB-	cetyltrimethylammonium bromide
DLS-	dynamic light scattering
DMEM-	Dulbecco's modified Eagle's medium
DMSO-	dimethyl sulfoxide
DNA-	deoxyribonucleic acid
EDC-	N-3-dimethylaminopropyl-N-ethylcarbodiimide hydrochloride
EDTA-	ethylenediaminetetraacetic acid
EPR-	enhanced permeability and retention
EtOH-	ethanol
FCS-	fluorescence correlation microscopy
GFP-	green fluorescence protein
GIT-	gastrointestinal tract
GO-	graphene oxide
$HAuCl_4$-	choloauric acid
HEPES-	N-2-hydroxyethylpiperazine-N'-2-ethanosulfonic acid
LB-	lysogeny broth
MTT-	3-(4,5-dimethylthiazol-2-yl)-2,5-diphenyltetrazolium bromide

$NaBH_4$-	sodium borohydride
NaCl-	sodium chloride
NHS-	N-hydroxysulfosuccinimide sodium salt
NIR-	near infrared
nm-	nanometer
NPs-	nanoparticles
PAC-	poly-alkyl-cyanoacrylates
PAMAMs-	Poly(amidoamine)
PBS-	phosphate buffered saline
PCL-	poly-ε-caprolactone
PDI-	polydispersity index
pDNA-	plasmid DNA
PEG-	polyethylene glycol
PEI-	polyethylenimine
PFA-	paraformaldehyde
PLA-	polylactic acid
PLGA-	poly(lactic-co-glycolic acid)
QDs-	Quantum dots
RES -	reticuloendothelial system
RNA-	ribonucleic acid
RNAi-	RNA interference
ROS-	reactive oxygen species
siRNA-	small interference RNA
SLN-	solid lipid nanoparticles
T/E-	trypsine/EDTA
TBE-	tris base EDTA buffer
TOAB-	tetraoctylammonium bromide
UV-Vis-	ultraviolet visible

W/O/W- water/oil/water

1. Introduction

Nanotechnology is a developing area in science and technology that is being widely explored during the last decade and is one of the most important areas related to drug delivery, cancer treatment and diagnosis. The potential of this field is applied to multiple circumstances and the opportunities to improve the current state of pharmaceutics are endless (1). The need for novel ways to efficiently deliver drugs was raised and nanocarriers are a possible answer to this problem. Capable of targeting delivery, the use of these carriers may diminish the amount of drug lost in nonspecific cells and tissue biodistribution, where some of them are rapidly cleared from the body (2). Nanoparticles appear as a possibility to alter the pharmacokinetic profile of drugs and their toxicity, improving the therapeutic index (3).

As drug delivery vehicles, it is expected that these carriers possess some characteristics like drug entrapment, immune system escape, extending the circulation time, targeting to the diseased site, avoiding most healthy organs and release the drug (4). These key factors allow the effective delivery of the drug to the target site.

The journey that a drug carrier has to pass from the moment where it is introduced in the organism until reaching the final target is complex, depending on many different factors. The interaction between the drug carriers and the reticuloendothelial system (RES) will determine if it will arrive to the final destination or not. It may be cleared by phagocytic cells as macrophages or filtered in the spleen or kidneys (5). Usually, the traditional drug delivery routes have a poor pharmacokinetic profile leading to a rapid clearance of the drug and therefore, requiring high dosages to intensify the effect and have a more efficient response.

If the carrier is able to overcome the steps that lead to poor biodistribution, it can adhere at the desired site in the vasculature or permeate through the vasculature until the desired site (5). Then diffusion of the carrier through the interstitial space and endocytosis can occur.

The physical and chemical characteristics of nanoparticles may affect their translocation through the biological barriers and distribution in the organism and also their toxicity (6, 7). These characteristics are size, shape, surface properties, surface coating, composition, solubility, aggregation/agglomeration, particle uptake, presence of transition metals related to the nanoparticles (7).

1.1 Size of nanoparticles

The size is directly related to the cellular uptake rate of the nanoparticles and to the circulation time it spends in the bloodstream (8). Smaller nanoparticles, less than 10nm in diameter, are believed to be cleared via glomerular filtration in the kidneys, whereas larger nanoparticles, more than 100nm, are probably cleared through the Kupffer cells in the liver and through the spleen (9). It has also been found that nanoparticles of size 40 to 50nm have a maximum uptake rate *in vitro* (10) while for *in vivo* studies the optimum size range is between 10 to 100nm (11). The effect of size in the cellular uptake was studied by Senior et al., who reported that liposomes with size greater than 400nm, were removed faster (0.2h) towards the liver than small vesicles, 200nm, that stayed more time in circulation through the blood stream (1.5h) (12, 13).

1.2 Shape of nanoparticles

The internalization and interaction of the nanoparticles is also very dependent on the shape that the nanoparticle acquires. Different shapes will generate different hydrodynamic forces and different motion through the vasculature and lead to specific trajectories (8). The symmetry of the particles will dictate if they are more effectively taken up, by accommodating better to the cellular membrane. Spherical particles have constant forces acting on themselves allowing the flow to happen without major interferences (14). However, asymmetrical particles, because of their shape, are subjected to different forces acting on them as well as resulting in considerable changes of trajectory relative to the main flow, ending up accumulating in the blood vessels walls (15). The circulation time also varies with the shape of the particles such as spherical particles that are cleared more rapidly than asymmetrical ones (14).

1.3 Surface charge of nanoparticles

Particles charge is important when considering their binding capacity towards the target site. The non-specific binding during the circulation is one of the factors that leads to poor bioavailability and to low efficiency rate. Positively charged nanoparticles will bind to anionic nucleic acids, proteins, glycans and phospholipids based groups situated on the cell surface, enhancing the cellular uptake due to the higher cellular binding (16). Negatively charged particles are taken up more efficiently than neutral particles (17). The clearance pathway will also be affected by the charge of the particles, positively charged particles will be cleared via the mononuclear phagocyte system and subsequently be

cleared more rapidly due to interactions with blood proteins, activating the complement pathway (8).

1.4 Hydrophobic/hydrophilic character of nanoparticles

Nanoparticles that are more hydrophobic than the cell surface will enhance the uptake and the amount of proteins linked to their surface (16). This characteristic will lead to more rapid clearing than hydrophilic particles that don't have the same amount of proteins binding to their surface and thus remain more time in circulation (8). It is now well known that polymers like polyethylene glycol (PEG) offer a hydrophilic surface to the particles, avoiding protein adsorption and delaying the clearance of the carriers (4).

1.5 Mechanical flexibility of nanoparticles

Flexible particles spend more time in circulation than rigid ones that can potentially clog the vessels if they are not small enough (4). These rigid particles were shown to be taken up by macrophages contrary to the soft particles that are not so susceptible of being adsorbed by these cells (18).

There are many factors that affect the design and final performance of nanocarriers, potentiating different interactions and making it impossible to predict every reaction and every factor that will be influenced in a determined system. It is of extreme importance to study these factors and to try experimentally to find answers for these nanoparticle systems.

1.6 Types of nanoparticles

In recent years, several nanocarriers have been developed with a wide range of characteristics as can be seen in Figure 1. In the following subsections, some of the most common nanoparticles used for drug delivery applications are described.

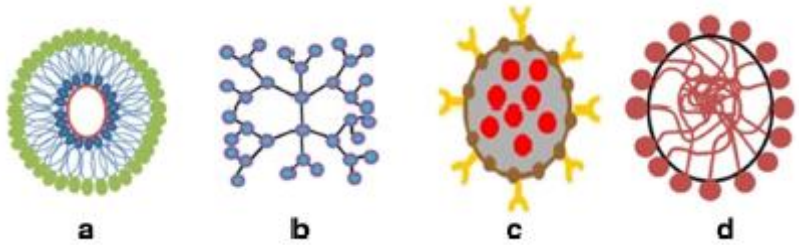

Figure 1. Some types of nanoparticles used for drug delivery: (a) liposome; (b) dendrimer; (c) functionalized polymer; (d) micelle. Adapted from Cole et al. 2015

1.6.1 Carbon-based nanocarriers

Carbon-based nanocarriers such as fullerenes, carbon dots, nanodiamonds and nanofoams are being investigated as a promising area of nanoparticles research and specially carbon nanotubes that are being suggested as drug carriers (5). These hollow cylinders are composed of rolled sheets of graphene and exhibit single or multi-walled morphology (19). They have unique structures and a specific combination of characteristics (mechanical, thermal, surface, optical, magnetic, electrical, chemical) that turns them ideal for *in vivo* drug delivery applications. Being flexible, they are able to penetrate cells and tissues. Regarding biocompability, it has been reported that they activate the complement system through classical and alternate pathways, inducing inflammation, oxidative stress, apoptosis, toxicity, lipid peroxidation, mitochondrial dysfunction, changes in cell morphology and platelet aggregation (20). For these reasons, the study of their toxicity is tremendously important and should be addressed with high priority. It has been concluded that it is necessary to make material modifications to fully avail the benefits of the carbon nanotubes-based biomaterials (21).
In recent years, Graphene Oxide (GO) has become a potential candidate for drug delivery applications. Graphene is a single layer sheet structure that naturally exists as graphite in bulk form (5). Modified GO has been used for targeted drug delivery and controlled release in tumor therapy (22). The effect of GO on cells revealed no cytotoxicity (23) even though it can cause oxidative stress and loss of cell viability depending on the size and concentrations used.

It is still needed to further study the biocompability of these nanoparticles prior to their use in clinical settings and find a compromise between the effective delivery of drugs and the systemic toxicity caused.

1.6.2 Dendrimers

Dendrimers are spherical branched structures composed of a core molecule and polymeric tree-like extensions that allow physical entrapment or encapsulation of pharmaceuticals (24). Their synthesis allows easy purification and a great control on the final characteristics. They are the smallest nanoparticle system, ranging between 2.5 to 8 nm (24). Dendrimers can have therapeutics attached to their branches via the functional groups, incorporated in the channels formed throughout the molecule or encapsulated in their core in case of an hydrophobic drug (25). In addition to drug encapsulation advantages, I-labelled anionic PAMAMs of lower generation also enhance the cellular

permeability improving oral drug delivery (26). Dendrimers can even act as natural antitumor, antiviral and antibacterial agents (27).

1.6.3 Lipid-based nanocarriers

Lipid based nanocarriers have also gain great attention for the drug delivery applications in recent years. Liposomes, one of the most used lipid-based nanocarriers, are generally composed of one or more bilayers of an aliphatic lipid molecule that forms a vesicle (5). These structures allow encapsulation of pharmaceutics inside the vesicle, entrapped by its layers. The advantages of these nanocarriers are easy functionalization, tunable surface properties and controlled size for specific drug delivery system (28). Liposomes are also known for activating the immune system, especially those with a positive surface charge (29). One of the downsides of liposomes is their selectivity with functionally compatible drugs, since the particles are unable to release sufficient amount of drug to be efficient as an antitumor agent, even after passive accumulation at tumor sites (5).
Other type of lipid-based nanocarriers are solid lipid nanoparticles (SLN). SLN are "colloidal particles of highly purified triglycerides, complex glyceride mixtures, or waxes stabilized by a surfactant" (30). They are produced by changing the oil phase of a oil/water emulsion for a solid lipid, allowing them to remain solid at room and body temperature (31). SLN are very popular as colloidal carriers because they allow controlled drug release and drug targeting, increasing the drug stability without inducing toxicity. In the designing of SLN, organic solvents can be avoided, and incorporation of lipophilic and hydrophilic drugs are enhanced (31). On the other hand, the disadvantages associated with SLN are the low drug loading and the polymorphic transition, which can lead to the expulsion of the drug from the carrier during the shelf-life of these systems (32).

Lipid-based nanocarriers are vulnerable to changes in temperature and osmotic pressure, being unstable in biological media, thus suggesting the need to use stable enhancing alterations (25).

1.7 Polymer based nanocarriers

Polymeric nanoparticles are comprised of a wide range of synthetic polymers, natural polymers and pseudosynthetic polymers (5). These nanoparticles are used as drug carriers thanks to their architecture, composition, stability and solubility (33). They have been described as excellent carriers because of their ability to provide protection to the drug, being able to release the encapsulated drugs in a controlled way and targeting them with a capacity for accumulation in the tumor site (33). Another advantage of these

nanoparticles is their ability to overcome poor solubility of some drugs and enhanced their biodistribution (34). These nanoparticles can take the shape of nanospheres or nanocapsules, on the first the drug is dispersed in the particle, while in the latter case, it is entrapped inside the vesicle and surrounded by a polymeric membrane (35). This nanocarriers system also allows the use of hydrophilic and hydrophobic drugs, attaching them to the nanoparticle's surface or encapsulating it inside their core.
The biodegradable polymers mostly used are poly(lactic-co-glycolic acid) PLGA, polylactic acid (PLA), poly-ε-caprolactone (PCL), poly-alkyl-cyanoacrylates (PAC) and chitosan (4).

PLA is a biocompatible and biodegradable polymer that is easily eliminated from the organism once it suffers scission into monomeric units of lactic acid (4). Xing et al. reported that oridonin PLA entrapped nanoparticles enhanced the solubility and extend the blood circulation time of this diterpenoid that induces cytotoxicity to a wide variety of cancer cells (36, 37).

PLC is particularly interesting for the preparation of long-term implantable devices thanks to its longer degradation time, comparing to polylactide (4). Several anticancer drug molecules used for cancer treatment had been studied by incorporation into PCL aiming to improve the therapeutic index of these molecules (38, 39).

PAC is a biodegradable and biocompatible polymer and when preparing the PAC nanoparticles several methods such as emulsion polymerization, interfacial polymerization and nanoprecipitation have been used for the preparation of PAC nanoparticles (40). The encapsulation of various antibacterials (ampicillin), anti-inflammatory (indomethacin) and anticancer drugs (doxorubicin and ftorafur) has been used for delivery using PAC nanoparticles which have shown the polymer to be a strong candidate for future investigations as a drug release vehicle (40).

Derived from the crustacean, natural biopolymer chitin, chitosan is a modified carbohydrate polymer that has successfully encapsulated several molecules for *in vivo* purposes (40). Chitosan nanoparticles have served as matrixes of a range of drugs from antihormonal (glycyrrhizin) to insulin, where the intestinal absorption following oral administration was enhanced; chitosan nanoparticles have also showed great results regarding drugs delivery to the ocular surface (40). De Campos et al. showed that chitosan NPs loaded with cyclosporin A can contact directly with corneal and conjunctiva surfaces, where the delivery is more effective and the inner ocular structures are not compromised, as well as, the systemic drug exposure is reduced (41).

1.7.1 Poly (lactic-co-glycolic acid) nanoparticles

Poly (lactic-co-glycolic acid) (PLGA) is a co-polymer widely used for drug delivery applications. The hydrolysis products of PLGA leads to form lactic acid and glycolic acid, which are metabolites, thus being considered a biodegradable and biocompatible polymer (42). The degradation time can vary according to the ratios of each monomer and molecular weight (43). These nanoparticles are believed to enter the cells by fluid phase pinocytosis and also through clathrin-mediated endocytosis, rapidly entering the cytoplasm escaping from the endo-lysosomes (43).

1.7.1.1 Methods of formulation of PLGA

These nanoparticles can be prepared by different methods, resulting in various structures and drug loading capacities. The drug can be encapsulated inside a core of a "nanocapsule" or entrapped or adsorbed in a matrix structure of a "nanosphere". Regarding PLGA nanoparticles, the most common technique is emulsification-solvent evaporation technique, where the polymer and the compound are dissolved in an organic solvent and then water and a surfactant are added to the polymer solution to form an oil/water emulsion. The nanosized droplets are formed by sonication or homogenization, the solvent is evaporated or extracted from the solution and the nanoparticles are collected after centrifugation (43). This method was recently altered to achieve a double water/oil/water emulsion (W/O/W) where it is possible to encapsulate hydrophilic drugs (peptides, proteins and nucleic acids).
Another technique used is the nanoprecipitation method/interfacial deposition method when the polymer and drug are dissolved in an organic solvent and then added dropwise to water, letting the organic solvent to evaporate and collecting the nanoparticles after centrifugation (44).

The spray-drying method is also becoming a popular method for the formulation of PLGA nanoparticles (45).

Drug loading can occur in two different phases of their production: incorporation of the drug during the nanoparticles (NPs) production or adsorption of the drug after the NPs production (43).

1.7.1.2 Physico-chemical properties of PLGA

PLGA NPs are often surface modified since the natural charge of PLGA NPs is negative and it has been shown that particles with cationic surface charge are easier to entering

through the cells (43). To assess the particle charge, the most common measurement performed is the zeta-potencial where the mobility of charged particles is monitored by an electrical potential. This measurement can be made using dynamic light scattering, where the Brownian motion of the particles causes dispersion of light and makes it possible to measure these fluctuations (46). The particles size and polydispersity index can also be measured using this technique. Other imaging techniques such as scanning or transmission electron microscopy or atomic force microscopy can also provide this information about the particles. The typical size of these particles is between 100 to 250 nm (43).

1.7.1.3 Encapsulation of small hydrophobic drugs in PLGA

Generally, the method used to incorporate hydrophobic poorly soluble drugs into PLGA NPs is by nanoprecipitation. To guarantee the drug release and the effective response of the NPs, several parameters are influential for the optimal performance, including surface modifications, the preparation method, particle size, the drug's molecular weight and the ratio of lactide to glycolide moieties used (40). PLGA NPs have been described as efficient nanocarriers for different anti-cancer agents such as paclitaxel (47), 9-nitrocamptothecin (48), cisplatin (49), and others, and even for several other drugs as haloperidol (50), estradiol (51), etc.

1.7.1.4 Encapsulation of proteins in PLGA

The oral bioavailability of proteins is very limited, since it is difficult for them to overpass the epithelial barriers of the gastro-intestinal tract (GIT), they are degraded by digestive enzymes, present a short half-life *in vivo* and difficulty in diffusion across some biological barriers (43). Encapsulating proteins inside PLGA NPs can be a promising solution for some of the above mentioned challenges. Encapsulation of proteins enables their protection against enzymatic and hydrolytic degradation, maintains their integrity and therefore, their activity, while their bioavailability could be improved (43). However, there are some problems that can occur during the nanoparticles preparation. The most utilized method for the encapsulation of proteins inside PLGA NPs is the double emulsion W/O/W solvent evaporation method since proteins are normally hydrophilic macromolecules. During this method, the proteins can be dissolved in the aqueous phase but can aggregate or denature at the water/organic solvent interface. They can also be adsorbed to the hydrophobic polymer or unfold because of the shear stress used during the method. If this happens, denatured or aggregated proteins can cause side effects like toxicity or

immunogenicity and induce the opposite reactions (52). For this reason, the protein stability is extremely important and is being studied for its improvement.

Another problem regarding protein stability is the exposure to an acidic environment, caused by the degradation products (lactic acid and glycolic acid) and by the carboxylic acid end groups that can interact with the positive charges of the encapsulated protein. This interaction can alter or block its release from the NP. The acidic pH can also lead to aggregation of the protein or affect its activity (53). Stabilizing agents such as pluranic F68, trehalose and sodium bicarbonate can increase the protein stability and are important tools to optimize this procedure (54).

1.7.1.3 Encapsulation of nucleic acids in PLGA

Nucleic acids are fragile, have a large size and are negatively charged leading to poor intrinsic transfection efficiency. In therapeutics, nucleic acids can promote gene expression by delivering a gene that is not present or not expressed (cDNA) or by silencing the expression of determined genes (RNAi mediators). The nucleic acids can be entrapped into the polymeric matrix or adsorbed by electrostatic interaction on the nanoparticle surface by adding surfactants or cationic polymers to it (55, 56). The W/O/W solvent evaporation method and the modified nanoprecipitation methods are used for the encapsulation of nucleic acids and there aren't visible major differences regarding the two methods used. By adding cationic polymers as polyethylenimine (PEI) (57) or chitosan (58), the encapsulation efficiency is augmented and the cellular uptake and endosomal escape are enhanced. Still, even with high encapsulation efficiency, the nucleic acid loading remains relatively low (0.1 to 1 mg per 100 mg of NPs) (43).

1.8 Metallic nanoparticles

Metallic nanoparticles have potential to be used as targeted drug delivery vehicles but also as imaging agents thanks to their unique physical and chemical properties that include plasmonic resonance and fluorescence enhancement as well as catalytic activity enhancement (59). The most used metals to form metallic nanoparticles are Iron, Zinc, Gold and Silver. These nanoparticles can carry large drugs doses and increase their circulatory half-life since they have a large surface area and area to volume ratio (59). Metallic nanoparticles have the ability to produce Reactive Oxygen Species (ROS) and this characteristic can be used to kill cancer cells (60). Regarding imaging abilities, their photoluminescence and superparamagnetic properties turns them into potential candidates for monitoring cancer treatment (61). Depending on the metal used, size and shape of the nanoparticle and its surface properties, there are several processes

described as potential procedures to kill cancer cells: hyperthermia, photothermal effect and ROS generation (59).
The synthesis processes used to form metallic nanoparticles vary from reduction, sonolysis, hydrothermal synthesis and pyrolysis (59). The size and shape will vary depending on the method used during their production, the best one should be considered depending on the final goal.

1.8.1 Gold nanoparticles

Gold nanoparticles (AuNPs) have unique physicochemical properties that distinguish them, their chemical inertness, facile surface functionalization, surface plasmon resonance and optical properties all of which turns them great candidates for drug delivery and imaging agents (62). AuNPs can be processed in to a wide range of sizes and shapes making them interesting for different approaches.
Hyperthermia can be induced by AuNPs, when radiation of near infrared (NIR) light is focused on these particles and because of its optical properties offers photothermal therapy for cancer therapy (62).

1.8.1.1 Synthesis methods of AuNPs

There are different synthesis methods for obtaining gold nanoparticles. Some of the most common methods are:

- Turkevich method (63) – reduction of Au^{3+} to neutral Au atoms using hot chloroauric acid reacting with sodium citrate. Gold starts to precipitate in the form of nanoparticles from the supersaturated solution
- Perrault method (64) – chloroauric acid is reduced by hydroquinone, which improves the monodispersity and shape consistency due to its weak reducing potential
- Block copolymer-mediated synthesis (65) – Au ions are reduced by block copolymers forming clusters whose surfaces are then reduced to grow the nanoparticle that are later stabilized
- Brust method (66) – Chloroauric acid reacts with tetraoctylammonium bromide (TOAB) that is a phase-transfer catalyst and stabilizing agent and with sodium borohydride that acts as reducing agent

Each method has different advantages and disadvantages and should be used depending on the final objective.

1.8.1.2 Therapeutic applications of AuNPs

Plasmonic gold nanoparticles can attach themselves to cancer cells via molecular targeting and delivered to tumor sites via the enhanced permeability and retention (EPR) effect (67). On accumulating at the tumor site, they can be triggered by external radiation and cause hyperthermia, leading to apoptosis. Another advantage of these particles is that they can be triggered by NIR light that passes easily through the epithelial tissue and causes minimal interference with water and hemoglobin (68).
The nanometer size and EPR within tumor site, allied to the facility to functionalize the surface chemistry of these nanoparticles with different biomolecules, turn them into ideal drug delivery candidates. Their ability to bind to drug molecules also enhances the drug efficiency and efficacy rate. The combination of all these characteristics, allows controlled drug release internally or externally, by biological stimuli or light activation (69). Therefore, AuNPs are undoubtedly excellent platforms for effective drug delivery.

There is another area where gold nanoparticles can offer a promising alternative, as nonviral gene delivery agents. By helping circumvent some of the barriers like cell membrane penetration, enzymatic degradation and the effective delivery of the gene to the nucleus, they can be a useful tool for gene regulation (69). Attaching DNA molecules to AuNPs may allow the knockdown of a gene of interest (70). Conjugating them with small interference RNA (siRNA) and exposing them to internal or external stimuli, the siRNA can be released and the RNA interference (RNAi) activity will increase, interfering with normal gene function (69).

1.9 Multifunctional nanoparticles

The development of “multifunctional” nanoparticles seeks to enhance benefits brought by nanoparticles combining different functionalities as improved delivery, imaging properties, targeting and therapeutic outcome (71). These nanoparticles offer a broad range of benefits and can overcome several challenges towards the improvement of the therapeutic index of the drugs used. The advantages of multifunctional nanoparticles include evading the immune system and preventing opsonization, preventing degradation of the protective cargo, targeting specificity, improved cell uptake and controlled drug release (71).
By combining therapeutic and diagnostic functions in a single nanoparticle, theranostic agents are formed, which can simultaneously deliver imaging and therapeutic benefits to specific sites or organs, allowing the detection and treatment of a disease to occur in a single procedure (72).

Ideal theranostic agents must accumulate rapidly and selectively, reporting biochemical and morphologic characteristics of the disease while efficiently delivering the drug that must be cleared rapidly from the body or be biodegraded into nontoxic byproducts that are safe for Humans (72). This is a trend to personalize disease management and to improve the efficacy lowering the toxicity and thus increasing the quality of life and patient outcome.

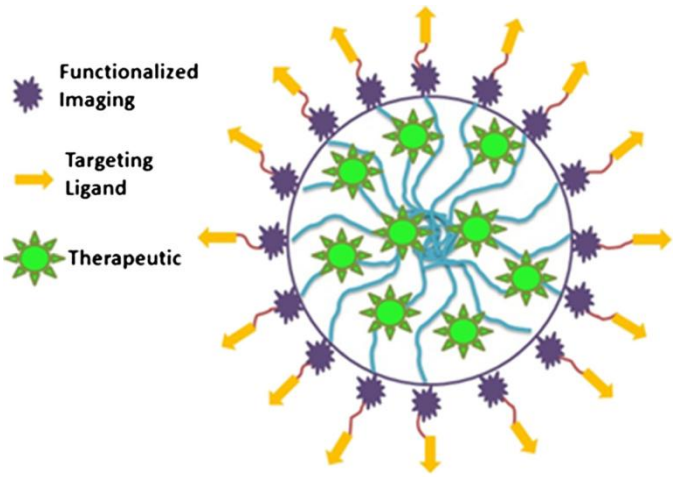

Figure 2. Scheme of a theranostic nanoparticle. Adapted from Cole et al. 2015

Although theranostic nanoparticles bring a lot of positive aspects, there are also some challenges that must be faced when considering these nanoparticles. By adding an imaging agent to a drug carrier, some imaging properties might be acquired but can be still below the threshold for images with sufficient quality and resolution. Another drawback might be the low drug loading capacity of nanoparticle-based imaging agents that only allow a small number of drug molecules to be incorporated per particle. For therapeutic purposes, a long circulation time is preferred to enhance tumor accumulation via EPR, but for imaging purposes, the contrast agent must be cleared rapidly to accurately evaluate the images of the site of interest. Therefore, a compromise between optimal features of both factors must be achieved, considering the increasing costs and complexity of synthesis and purification steps when adding more features to the particles, forming more heterogeneous formulations (71). The response for this challenge might be the use of nanomaterials that exhibit an intrinsic utility for both imaging and therapy. Some examples include iron oxide nanoparticles, which are ideal both for MR imaging and thermal ablation therapy (73), gold nanoparticles for computer tomography (CT), imaging and radiation therapy (74) and even for CT imaging and thermal ablation therapy (74). These nanoparticles, when irradiated with the appropriate form of energy, absorb the incident energy and convert it to heat, which kills the cancerous cells (71). The most

common energy sources used are near infrared light, radiowaves or an alternating magnetic field (71).

Still, at the moment, the overall point of view considers that addition of targeting ligands to therapeutic nanoparticles is worth the additional complexity of synthesis, cost and regulations (71).

1.10 Stimuli-responsive nanocarriers

The nanotechnology-based targeted delivery is evolving rapidly, aiming to overcome the difficulties to control the release of the drug from the targeting nanocarrier. A solution seems to possibly be on-demand processes (also known as “switch on/off”) that allow tailored-release profiles with excellent temporal, spatial and dosage control (75). When designing the stimuli-responsive systems, the microenvironment of the release should be recognized by the nanocarrier and it should act in a dynamic way, mimicking the organism behavior. The materials used should be biocompatible and have specific characteristics that enables it to undergo specific protonation, hydrolytic cleavage and molecular or supremolecular conformational change when responding to a specific stimuli, or being susceptible to specific physical stimulation (75).
Nanodelivery systems may be susceptible to different types of stimuli, being exogenous or endogenous. As exogenous stimuli, there are thermoresponsive systems, magnetically responsive systems, ultrasound-triggered drug delivery, light-triggered drug delivery and electroresponsive systems. Regarding endogenous stimuli, there are different approaches under study, some of them include pH-sensitive systems, redox-sensitive systems, enzyme-sensitive systems and self-regulated systems (75).

The wide range of stimuli that can trigger the drug release from a nanocarrier at the right time and place allows great flexibility and diverse responses to problems regarding the release of the therapeutic. Although the complexity of their designing and synthesis makes it difficult to scale up and transfer the technology from the laboratories to their mass use, the developments made in this field of research offer a great potential.

1.11 Scope and aims

The potential of this field to improve the current state of pharmaceutics is enormous and the interest to explore is big.
Following this thought, the development of nanocarriers that can offer multiple advantages and a wide range of solutions for drug delivery and imaging properties is interesting and

provides challenges and great benefits if well accomplished. Therefore, the aim of this thesis was to design a nanocarrier capable of transporting a therapeutic agent while providing imaging information regarding the environment of the cancer site.

PLGA nanoparticles and AuNPs were developed with the aim to form a multiple functional nanoparticle, capable of therapeutic effect by transferring light triggered to heat, offering targeted treatment. The nanoparticles were developed and their toxicity, transfection and microscopy assays were performed in order to evaluate the nanoparticles' characteristics and evaluate their therapeutic potential.

2. Materials and Methods

2.1 Buffers

2.1.1 Hepes buffer

Hepes buffer solution of 20 mM concentration at pH 7.2 was made by dissolving 1.19 g Hepes (Sigma-Aldrich, USA) in 250 mL of deionized water.

2.1.2 TBE buffer

TBE buffer was made with 10.8 g of Tris base (Sigma-Aldrich, USA), 5.5 g boric acid (VWR International, USA) and 4 mL of EDTA pH 8.0 (Merck, Germany) dissolved in 1 L of deionized water.

2.1.3 Flow buffer

This is a buffer used for samples ready to analyse with flow cytometry. Sodium azide used to prevent microbial growth and fix the cells (inhibit their energy dependent activities). Flow buffer was made adding 0.1% Sodium azide (Sigma-Aldrich, USA) and 1.0% Bovine Serum Albumin (BSA) (Sigma-Aldrich, USA) to 500 mL of Phosphate-buffered saline (PBS) (Gibco, VS).

2.2 Chemicals

The chemicals chloroauric acid ($HAuCl_4$), sodium citrate ($C_6H_5Na_3O_7$), sodium borohydride ($NaBH_4$), PLGA, (N-3-Dimethylaminopropyl-N-ethylcarbodiimide hydrochloride) EDC, (N-Hydroxysulfosuccinimide sodium salt) NHS, chitosan, protamine sulfate salt, isopropanol, 3-(4,5-dimethylthiazol-2-yl)-2,5-diphenyltetrazolium bromide (MTT) and Trypan Blue were all purchased from Sigma-Aldrich, USA.

The Dulbecco's modified Eagle's medium (DMEM) and agarose were obtained from Invitrogen, LifeTechnologies (Carlsbad, USA). The acetone was obtained from Fisher Chemical and the sodium chloride (NaCl), yeast extract and tryptone from International Medical. OptiMEM reduced serum medium was purchased from Gibco,VS.

QIAGEN QIAfilter Gigakit was obtained from Qiagen®, Venlo, The Netherlands. The plasmid constructs gWIZ-GFP (Promega, Leiden, The Netherlands) were amplified in transformed *E. coli* bacteria. Alexa647-siRNA was purchased from Eurogentec, Seraing, Belgium.

2.3 Equipments

- Flow cytometer FACS Calibur, BD Biosciences Benelux N.V., Erembodegem, Belgium
- Microscope Nikon TE200E, NIKON BELUX, Brussels, Belgium
- Confocal laser scanning microscope, MRC1024 UV, Bio-Rad, Hemel Hempstead, UK
- Plate spectrophotometer Perkin Elmer 2104 Envision
- Ultracentrifuge, Beckman Coulter
- UV-Vis spectrophotometer Nanodrop 2000 C Spectrophotometer, Thermo Fisher Scientific, Rockford, IL, USA
- Zetasizer Nano Series, Malvern Instruments, Hoeilaart, Belgium

2.4 Preparation of gold nanoparticles (AuNPs)

The AuNPs were prepared using different reducing agents, concentrations and temperature conditions. The nanoparticles that were considered promising and showed reproducibility and stability over time are described.

2.4.1 Preparation of AuNPs using sodium citrate as reducing agent

Sodium citrate is known as an effective reducing agent and is widely used for the preparation of gold nanoparticles (63). The synthesis reaction was performed using 1 mL of $HAuCl_4$ solution of 1 mg/mL and 1 mL of MiliQ Water to which 1 mL of Sodium citrate solution of 1 mg/mL was added. The solution was stirring at 200 rpm (VWR VS-C4, USA) for 5 min at room temperature.

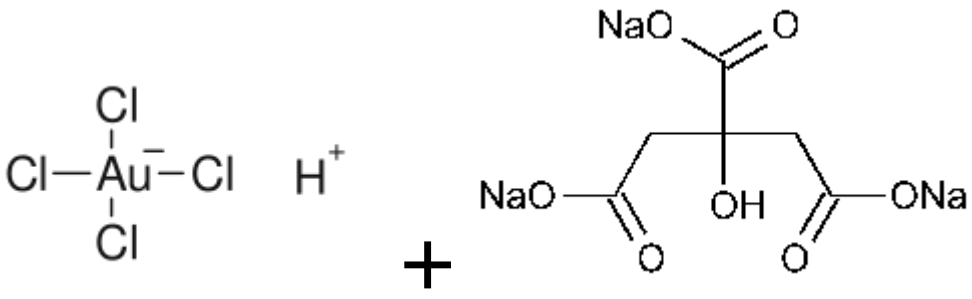

Figure 3. Structural formula of HAuCl4 and Sodium citrate

The same experiment was performed with the solution at 90°C and stirring at 500 rpm (IKA® RCT basic) for 5 min.

2.4.2 Preparation of AuNPs using sodium citrate and sodium borohydride

$NaBH_4$ is an inorganic compound used as reducing agent for several reactions. It has also been used to synthesize gold nanoparticles reducing $HAuCl_4$. Both the reducing agents were used with the aim to obtain reproducible and stable gold nanoparticles. Both ratios of reagents and temperature conditions were also varied.

2.5 Preparation of PLGA – poly(lactic-co-glycolic acid) Nanoparticles

2.5.1 Preparation of PLGA NPs

The PLGA NPs were prepared adding 40 mg of PLGA to 5 mL of acetone. This solution was stirred for 20 min at 200 rpm (VWR VS-C4, USA). After 20 min, the PLGA solution was added dropwise to 20 mL of MiliQ Water using a syringe and needle (Figure 4). This solution was stirred at 500 rpm for 10 min and kept overnight to remove acetone by evaporation.

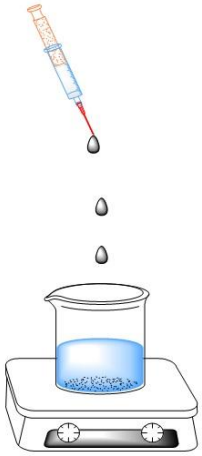

Figure 4. Addition of the PLGA solution dropwise to water, forming the nanoparticles

2.5.2 Preparation of PLGA NPs conjugated with chitosan and protamine

The positively charged NPs were made using the 8 mg/mL PLGA NPs described in 2.3.1 and adding 0.5 mM of EDC (N-3-Dimethylaminopropyl-N-ethylcarbodiimide hydro-chloride) and 0.25 mM of NHS (N-Hydroxysulfosuccinimide sodium salt). The chitosan and protamine were conjugated to the PLGA NPs by using carbodiimide chemistry (NHS/EDC) (76). Briefly, the PLGA NPs were activated by EDC/NHS and added dropwise to a solution of 1 mg/mL of Chitosan or Protamine. They were allowed to stay at room temperature stirring for 20 min. The modified PLGA based nanoparticles were

centrifuged at 10 000 rpm for 15 min at 15°C using an Ultracentrifuge (Beckman Coulter) to eliminate unreacted chitosan or protamine.

2.5.3 Preparation of PLGA NPs with Quantum Dots (QDs)

The QDs used were FL59: flash CdSe/CdS core-shell QDs with size of 13.4 nm and quantum yield of 70%. They have been previously prepared and for this study an aliquot of the QDs solution was used (77).
The PLGA NPs with QDs were prepared by mixing 20 mg of PLGA in 2.5 mL of acetone with different amounts of QDs (2, 4, 6, 8, 10, 20, 30, 40 and 50 µL). This solution was stirred for 20 min at 200 rpm (VWR VS-C4, USA) and was subsequently added to 10 mL of MiliQ Water. For the preparation of the positively charged PLGA NPs with QDs, the same procedure as described in 2.4.2 was followed.

2.6 Dynamic light scattering (DLS) of the NPs

Dynamic light scattering (DLS), a non-invasive technique, was employed to characterize the size and surface charge of the particles by measuring the hydrodynamic diameter, polydispersity index (PDI) and zeta-potential using a Zetasizer Nano Series (Malvern Instruments, Hoeilaart, Belgium). The particles suspensions were added into the disposable folded capillary cell DTS 1070. Measurements were carried out at temperature of 25°C and scattering angle 173°. All samples were measured in triplicate.

2.7 UV-Visible absorption of the NPs suspensions

Nanoparticles have optical properties that are sensitive to size, shape, concentration, agglomeration state and nanoparticle surface, which makes UV-Vis spectroscopy a valuable tool for identifying, characterizing, and studying these materials. Gold nanoparticles strongly interact with specific wavelengths of light and the unique optical properties of these materials are the foundation for the field of plasmonics.

2.8 Plasmid Purification

QIAGEN plasmid purification protocols are based on a modified alkaline lysis procedure, followed by the binding of the plasmid with QIAGEN Anion-Exchange Resin, with low-salt and appropriate pH conditions. All the non-desired molecules (RNA, proteins, dyes and low-molecular-weight impurities) are removed when the medium-salt wash is performed. The plasmid DNA is eluted in a high-salt buffer and by isopropanol precipitation it is

concentrated and desalted. Each disposable QIAGEN-tip packed with QIAGEN Resin should be used by gravity flow.

The plasmid multiplication in bacteria occurs when 1 or 2 bacteria beads are added to falcon tubes (Corning Incorporated) containing Lysogeny Broth (LB) medium (10 g of NaCl, 5 g of Yeast extract, 10 g of Tryptone diluted in distilled water to 1 L) with Ampicilin and are incubated at 37°C for 8 h at 250 rpm (New Brunswick Scientific). After 8 h of incubation, the bacteria culture is transferred to an Erlenmeyer with 800 mL of LB medium and incubated again at 37°C and 300 rpm for 12-16 h. On the day after, the bacteria suspension is transferred to centrifuge flaks (Corning Incorporated) and centrifuged for 15 min at 4°C at 6000 g.

The bacteria lysis is made by ressuspending the pellets in 125 mL of P1 buffer, then transferring it to Schot bottles and adding 125 mL of P2 buffer, incubating for 5 min for the cells to lyse, adding then 125 mL of P3 buffer and mixing gently. The lysate clearance is made using the QIAfilter cartridge with a QIAGEN tip and QBT buffer by gravity flow.

After the filtered lysate is poured in the QIAGEN tip, the ion exchange chromatography is performed washing the tip with QC buffer and then eluting the pDNA from the QIAGEN tip with QF buffer.

The precipitation and washing of the pDNA occurs when the eluted pDNA is divided to small centrifuge tubes with 0.3 volumes of isopropanol and incubated for 1 h at -20°C, being subsequently centrifuged for 30 min at 14 600 g at 4°C. The pellet is washed with 5 mL of ice cold 70% EtOH, centrifuged for 10 min at 15 000 g and 4°C and then air-dried at -20°C for 2-5 min. The pellet is then ressuspended with 500 µL of HEPES, transferred to eppendorf and stored at -20°C.

2.9 Gel Electrophoresis of the nanoparticles complexed with pDNA

Lipoplexes corresponding to 50 ng pDNA were prepared as previously described, after which 5 µL of Ambion loading buffer (Ambion, Merelbeke, Belgium) was added to the suspension. The mixture was loaded on a 1% agarose gel in 1 x TBE buffer, to which GelRed (Biotium, Hayward, CA) was added for visualization of the pDNA. The gel was run for 40 min at 100 V and imaged.

2.9.1 Complexation of the cationic nanoparticles with pDNA

The complexation between pDNA and cationic NPs occurs via electrostatic interaction, the negatively charged nucleic acid forms an electrostatic bond with the positively charged

NPs. The study of the complexation potential is interesting to evaluate the efficiency of the NPs to be used as gene therapy carriers.

The complexes were made using different volumes of nanoparticles represented in Table 1, which correspond to the concentrations displaced in Table 2. The concentration of pDNA was kept constant (1 µg/µL) for all the samples. The complexes were allowed to stay at room temperature for 20 min before being transferred to the gel electrophoresis.

Table 1. Complexation volumes used for gel electrophoresis

NPs volume (µL)	Hepes buffer (µL)	pDNA (µL)	Loading buffer (µL)	Total volume (µL)
1	18	1	5	25
5	14	1	5	25
10	9	1	5	25
15	4	1	5	25
17	2	1	5	25
19	0	1	5	25

Table 2. Complexation concentrations used for gel electrophoresis

Chitosan coated PLGA NPs (mg/mL)	Protamine coated PLGA NPs (mg/mL)	Chitosan coated PLGA QDs NPs (mg/mL)	Protamine coated PLGA QDs NPs (mg/mL)
0.4	0.9	0.1	0.2
0.8	1.8	0.6	0.8
1.6	3.6	0.8	1.2
2.4	5.4	1	2
3.2	7.2	-	-
4	9	-	-

2.10 Cell culture for cytotoxicity and transfection evaluation

The experiments to evaluate cytotoxicity and transfection efficiency were performed with HeLa cells, a human cervix carcinoma cell line. These cancer cells were the first immortalized human cell line to be grown in tissue culture and are derived from cervical

cancer cells from Henrietta Lacks, a patient suffering from this cancer (78). These cells are able to grow and adhere at plastic surfaces, becoming easily attached to culture flasks, allowing their use and easy maintenance. The materials used for cell culture experiments are from Invitrogen, Life Technologies (Carlsbad, USA), unless stated otherwise.

The cell culture medium used during the experiments was Dulbecco's Modified Eagle's Medium (DMEM) F12 containing 10% Fetal Bovine Serum, 435 mL DMEM F12, 10 mL Penicillin/streptomycin (100 IU/mL penicillin & 100 µg/mL streptomycin), 5 mL L-Glutamin 2 mM. The medium was filtered (Corning Incorporated, USA) using a vacuum system and the cells were incubated in culture flasks (SPL Life Sciences, Korea) at 37°C and 5% CO_2.

For maintaining the cell culture, the cells were trypsinized once they reached a confluency of 80-90%. All the medium was removed from the confluent flask and the cells were washed once or twice (according to the amount of dead cells) with ~10 mL of PBS. 3 mL of Trypsine/EDTA (T/E) at 0,25% was added to the flask and the cells were incubated for 5 min at 37°C with 5% CO_2. After the cells were detached, cell culture medium was added to the flask to neutralize the T/E. The cell suspension was transferred to a falcon tube and centrifuged at 1100 rpm for 7 min. After centrifugation, the pellet containing the cells was ressuspended in new cell culture medium and a certain quantity of this cell suspension was transferred to a new flask with culture medium.

To count the cells for every experiment, after trypsinization, 50 µL of the cell suspension was transferred to an eppendorf and 100 µL of Trypan blue was added. From this eppendorf, 10 µL were transferred to each side of Bürker counting chamber. The cells were counted on the microscope and calculations were made afterwards to obtain the final number of cells per mL.

2.11 Cell viability assay: MTT assay

The cell viability of the NPs was assessed by MTT assay. The MTT is a colorimetric assay for accessing cell metabolic activity using the tetrazolium dye MTT 3-(4,5-dimethylthiazol-2-yl)-2,5-diphenyltetrazolium bromide, which is reduced by NAD(P)H-dependent cellular oxidoreductase enzymes to its insoluble formazan, (E,Z)-5-(4,5-dimethylthiazol-2-yl)-1,3-diphenylformazan (Figure 5).

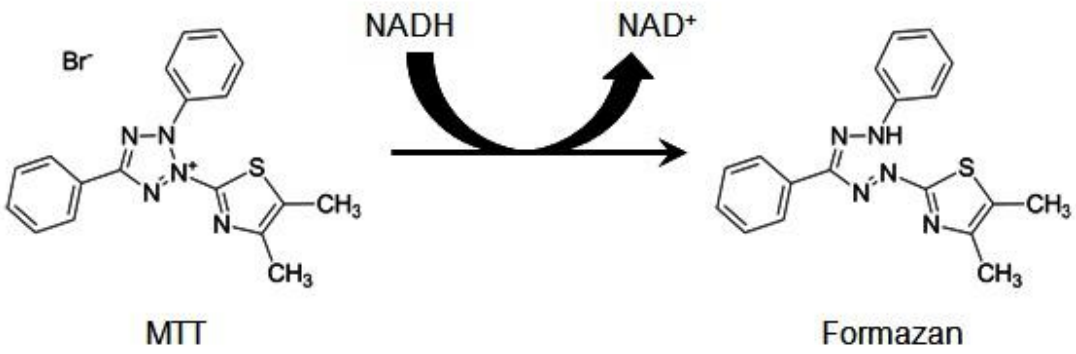

Figure 5. Structures of MTT and colored formazan product. Adapted from Riss et al. 2004

MTT is a yellow tetrazole reduced to purple formazan in living cells (79). Dimethyl sulfoxide (DMSO) is used to dissolve the insoluble purple formazan product into a colored solution. To know the absorbance of this colored solution, a spectrophotometer is used and the wavelength is chosen (usually between 500 nm and 700 nm). By this measurement it is possible to determine the amount of viable cells (79).

This assay was performed in two days, on day one the HeLa cells were seeded with a density of 50 000 cells/well in 24 wells cell plates. Then 5 mg/mL MTT solution was prepared in PBS. Different concentrations of NPs were used to observe cytotoxicity. After having all the NPs prepared and the cells with an optimal confluence of 50-60%, the cells were washed with OptiMEM and 450 µL of OptiMEM was added with 50 µL of particles in each well. Following 4 hours of incubation at 37°C and 5% CO_2, the OptiMEM and particles were removed, the cells were washed again with OptiMEM and then 400 µL of fresh culture medium (DMEM F12) was added to each well with 100 µL of MTT reagent. The negative control was done by fixating the cells with Paraformaldehyde (PFA) 4% for 15 min. The cells with the MTT reagent were incubated for 3 hours at 37°C and 5% CO_2. After 3 hours, the solution was removed and 500 µL of DMSO (Sigma-Aldrich, USA) was added to each well. The plates were covered with aluminum foil and placed on an orbital shaker for 45 min at 1200 rpm. The UV absorbance at 590 nm and 690 nm was made using a plate reader (PerkinElmer 2104 EnVision).

2.12 *In vitro* Transfection of NPs complexed with pDNA

To assess the transfection efficiency of particles complexed with pDNA, the following procedure was performed:

- The cells were spliced and seeded with a density of 50 000 cells per well.
- After 24 hours, the complexes were prepared according to the following protocols. The pDNA was diluted in HEPES buffer 20 mM pH 7.2 (1µg pDNA per well) and then in OptiMEM, and the nanoparticles were diluted to obtain the same concentrations tested in the toxicity assay. The nanoparticles were diluted in OptiMEM and then mixed with the pDNA and incubated at room temperature for 20 min. After that, the complexes were added to the cells, 500 µL to each well. Incubation occurred for 24 hours at 37°C and 5% CO_2, and the culture medium was refreshed after 4 hours. A positive control with Lipofectamine ^{TM} was used.
- After 24 hours of incubation, the cells were washed with PBS and trypsinized with 100 µL of T/E for 5 min at 37°C and 5% CO_2 after which 400 µL of cell culture medium was added to each well. The cell suspension was centrifuged at 1300 g for 6 min. The supernatant was discarded and the pellet dissolved in 300 µL of flow buffer. The transfection efficiency was measured on FACS for green fluorescence using FACSCalibur and all the data was collected using Cell Quest Pro (Beckton Dickinson, Erembodegem, Belgium).

2.13 Evaluation of NPs diffusion by single particle tracking (SPT)

The diffusion of NPs was measured using SPT. The NPs were diluted to a suitable concentration (10^8 to 10^{10} particles/mL) in HEPES buffer (25 mM, pH 7.2). The NPs solution of 9µL was applied between a microscope slide and a cover glass with a double-sided adhesive sticker of 120 µm thickness in between (Secure-Seal Spacer; Molecular Probes, Leiden, The Netherlands). The microscope was always focused at 5 to 10 µm above the cover glass. For each sample, typically 10 to 20 movies of about 200 frames each were recorded at different locations within the sample, at a frame rate of 24 or 35 fps depending on the exposure time. All fluorescence video imaging of diffusing nanoparticles was performed on a custom-built laser wide field fluorescence microscope setup. Diffusion analysis of the videos was performed offline using in-house developed software, providing a distribution of apparent diffusion coefficients from which hydrodynamic diameter could be calculated.

2.14 Evaluation of siRNA release from the NPs by fluorescence correlation spectroscopy (FCS)

siRNA release from the nanoparticles was determined by fluorescence correlation spectroscopy. FCS measurements were performed on a MRC1024 Bio-Rad confocal laser scanning microscope equipped with a water immersion objective lens (Plan Apo 60X NA, 1.2, collar rim correction, Nikon, Japan) and on an LSM510/ConfoCor2 system (Carl Zeiss, Jena, Germany), equipped with a type C-Apochromat 40x/1.2 W objective lens. The laser beam was focused at about 100 µm above the bottom of a 96-well plate (Greiner Bio-one, Frickenhausen, Germany) which contained the samples.

3. Results

3.1 Gold nanoparticles

3.1.1 Dinamyc Light Scattering (DLS)

Gold nanoparticles (AuNPs) have attracted much interest in therapeutic research due to its physiochemical properties. Many applications of AuNPs depend on three key parameters such as size, shape and monodispersity, which can be controlled during synthesis process. The citrate caped AuNPs are most commonly used. In the present study, we have investigated how the size of the AuNPs varies by concentration of $HAuCl_4$, reducing agent and applying co-reducing agent. The size of synthesized AuNPs particle is represented in Table 3. The formation of the AuNPs was confirmed by UV spectrum shown in Figure 6. The obtain results show that stable AuNPs can be designed at room temperature by using co-reducing agent. The AuNPs size can vary by changing the concentration of the $HAuCl_4$ and reducing agents.

Table 3. Results of the size measurements of different AuNPs formed in different conditions using DLS

Composition	Size (d.nm)	PDI	Temperature conditions
1 mL $HAuCl_4$ + 1 mL H_2O + 500 µL Sodium citrate + 200 µL $NaBH_4$	41.095 ± 1.3	0.197	Room temperature
1 mL $HAuCl_4$ + 1 mL H_2O + 1 mL Sodium citrate + 100 µL $NaBH_4$	17.83 ± 5.6	0.199	Room temperature
1 mL $HAuCl_4$ + 1 mL H_2O + 1 mL Sodium citrate + 50 µL $NaBH_4$	18.6 ±10.5	0.258	Room temperature
1 mL $HAuCl_4$ + 1 mL H_2O + 500 µL Sodium citrate	154.35 ± 32.2	0.158	Room temperature
1 mL $HAuCl_4$ + 1 mL H_2O + 500 µL Sodium citrate	61.875 ± 4.9	0.272	90°C

3.1.2 UV-Vis absorption of gold nanoparticles

The UV-Vis absorption spectrum of the solution showed that the absorption peak was between 510-540 nm, as expected to confirm the presence of AuNPs in the solution.

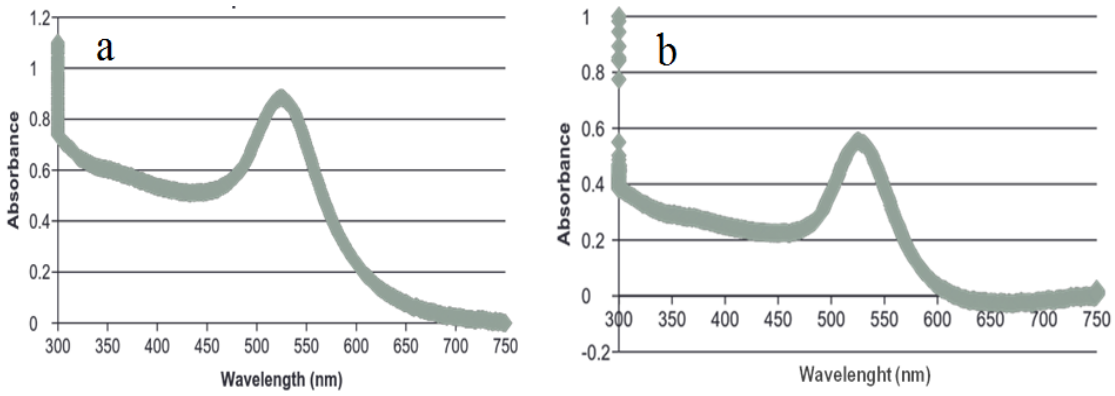

Figure 6. UV-Vis spectrum of AuNPs reduced with Sodium citrate (a); UV-Vis spectrum of AuNPs reduced with Sodium citrate and NaBH4 (b)

3.2 PLGA nanoparticles

3.2.1 DLS of PLGA NPs

The NPs biodistribution and pharmacokinetic properties are largely dependent on their size, surface charge and composition. To obtain various sizes of PLGA NPs, different concentrations of the PLGA solution was used. The results indicate that the size of PLGA NPs increased with increasing the concentration of the PLGA solution (Figure 7).

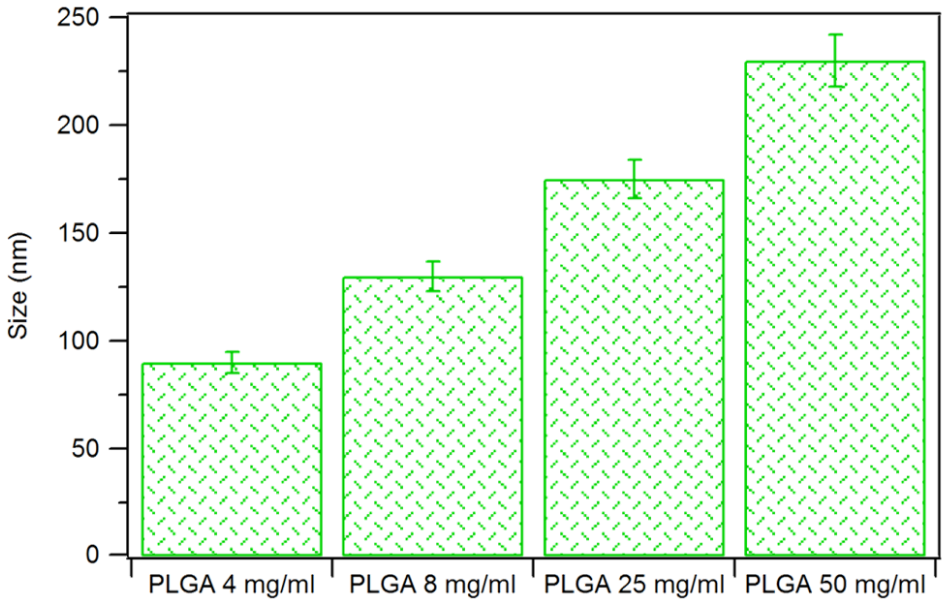

Figure 7. Sizes of different PLGA NPs with different concentrations of PLGA solution

From here onwards we focused only on 175 nm sized particles for further study. The centrifugation stability of the PLGA NPs was evaluated by measuring size and surface charge before and after centrifugation.

This new preparation method developed for PLGA NPs showed small variance of size and surface charge before and after centrifugation, shown in Figure 4.

3.2.2 Surface modification of PLGA NPs

The surface modification of PLGA NPs is a versatile approach to enhance its therapeutic applications. In the present study, cationic polymers chitosan and protamine have been chosen, for surface modification, which can improve biodistribution and pharmacokinetic properties of NPs (80, 81). The carboxylated PLGA NPs were conjugated to the amines of chitosan and protamine via carbodiimide chemistry. It was observed that NPs, when positively coated increased in size specially upon coating with chitosan in comparison to protamine (Figure 8). The coating of chitosan forms a layer on the nanoparticles which contributes to the increase in size.

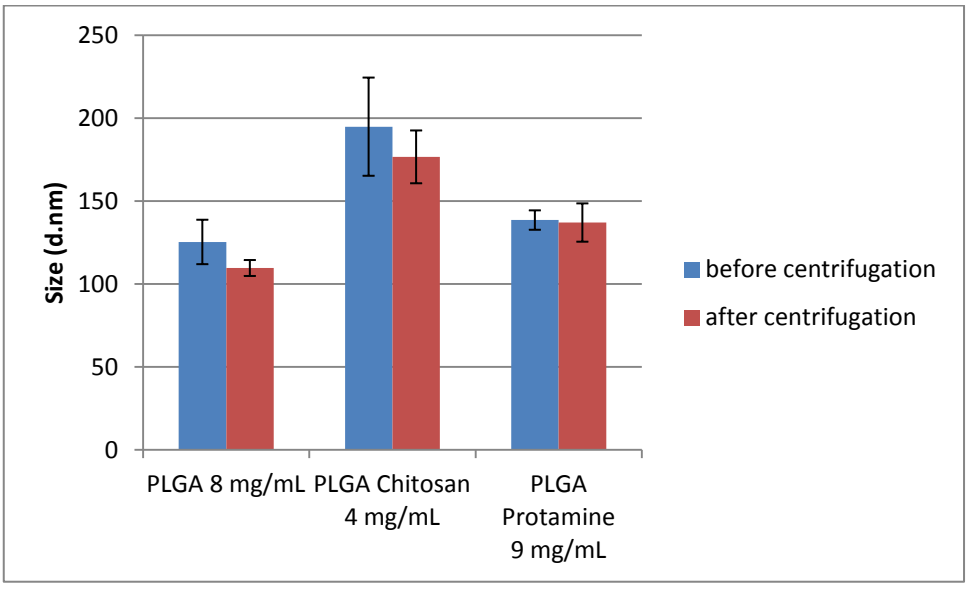

Figure 8. Average size of PLGA NPs and PLGA NPs positively coated with Chitosan or Protamine

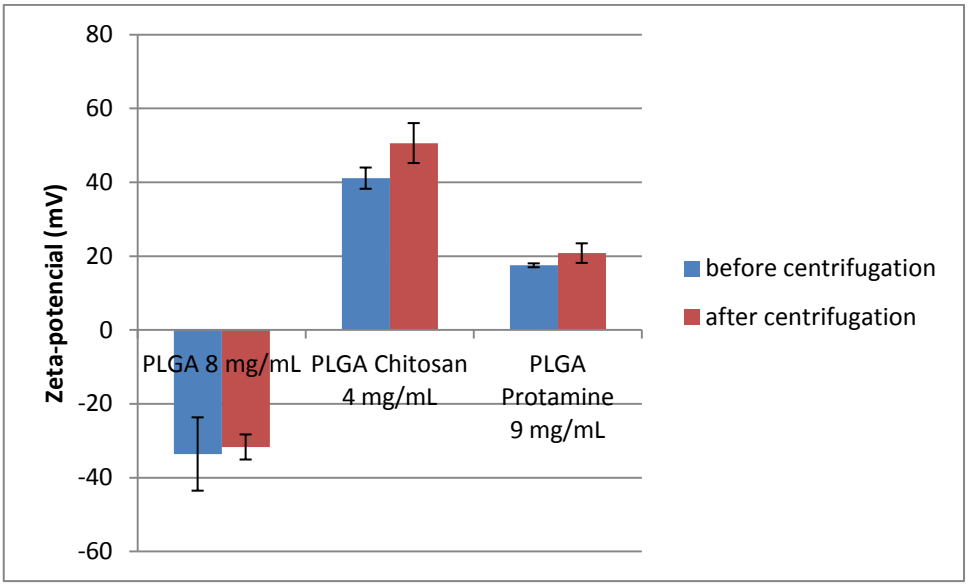

Figure 9. Average Zeta-potencial of PLGA NPs and PLGA NPs positively coated with Chitosan or Protamine

The change of the surface charge of the nanoparticles when coated with chitosan or protamine are presented in Figure 9. By comparing the two polymers coatings, it was observed that chitosan provides higher positive charge compared to protamine.

3.3 Evaluation of complexation potential between pDNA and cationic PLGA NPs by gel electrophoresis

The complexation between pDNA and cationic PLGA NPs occurs via electrostatic interaction, the negatively charged forms the electrostatic bond with the positively charged NPs. The complexation is further evaluated by gel electrophoresis method, where an electric field is applied to gel loaded with complexes. The molecules having a negative charge migrate towards the positive pole and negatively charged will move towards positive pole according to their size. The smaller the molecule, the faster is its migration. According to this phenomenon the complexation behavior can be studied. If the pDNA is well complexed with cationic PLGA NPs then the migration will be slower or there will be no migration at all in comparison to free pDNA which will migrate faster and further. The complexation ability of the different concentration of cationic PLGA NPs is shown in Figure 10 and in Figure 11.

3.3.1 Complexation potential between pDNA and chitosan coated PLGA NPs

Gel electrophoresis of pDNA complexed with different concentrations of chitosan coated PLGA NPs is shown in Figure 10. The results indicate that the concentration of 2 µg of

chitosan coated PLGA NPs doesn't show good complexation. The NPs concentration 8 µg onwards shows good complexation ability.

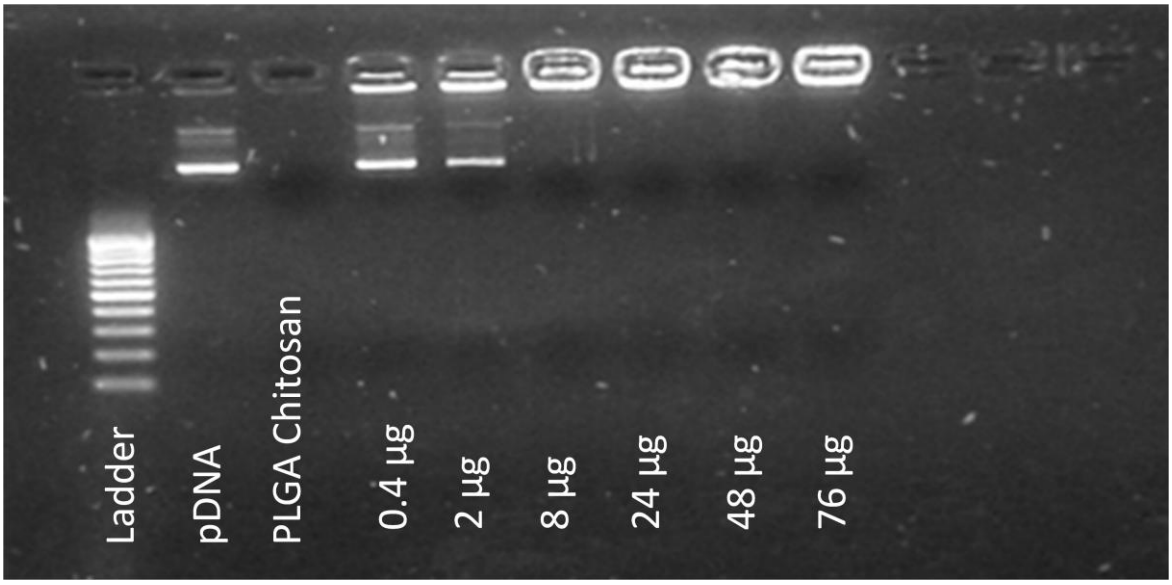

Figure 10. Photo of Gel Electrophoresis of pDNA with PLGA Chitosan NPs

3.3.2 Complexation potential between pDNA and protamine coated PLGA NPs

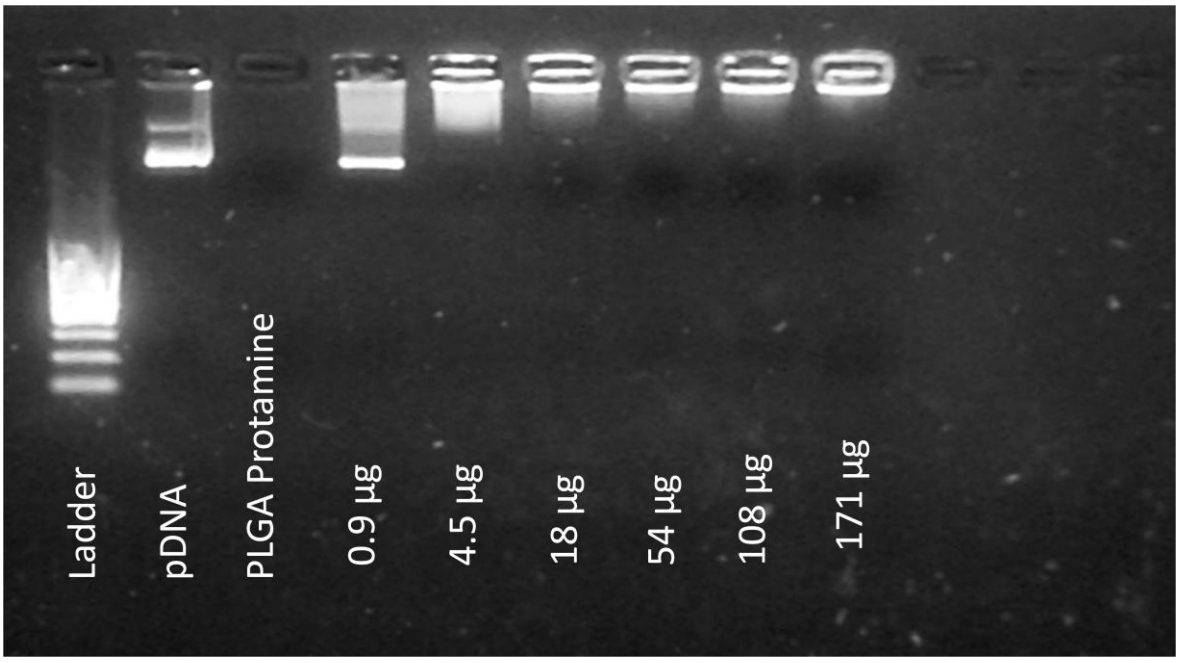

Figure 11. Photo of Gel Electrophoresis of pDNA with PLGA Protamine NPs

The protamine coated cationic PLGA NPs shows complete complexation at NPs concentration of 18 µg onwards.

3.4 Cytotoxicity evaluation of NPs

3.4.1 Cytotoxicity of PLGA NPs

The viability of HeLa cells after being exposed to PLGA NPs is shown in Figure 12. Different concentrations were evaluated and the results were compared with the positive (Blanc+OptiMEM; Blanc+CCM) and negative (Dead cells) controls. It was observed that up to 400 µg of NPs are considered non toxic to the cells. In the present experiment there were observed some unexpected result with 40 µg and 265 µg of NPs, which showed toxicity, the reason might be some kind of contamination during the procedure. Each sample was performed in triplicates and the assay repeated at least three times. The Figure 12 shows the average values of all assays.

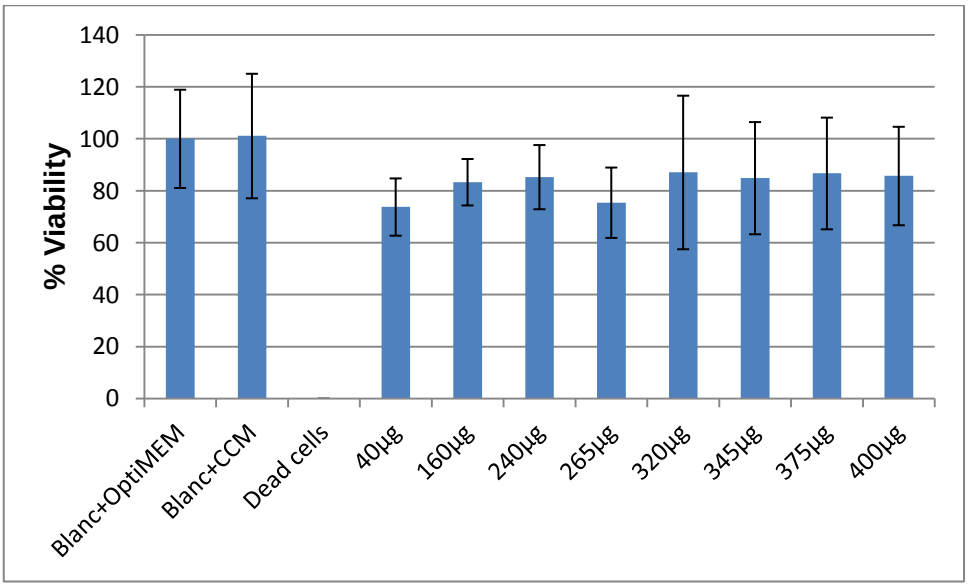

Figure 12. Percentage of viability of HeLa cells after exposure to PLGA NPs

3.4.2 Cytotoxicity of chitosan coated PLGA NPs

The chitosan coated cationic PLGA NPs did not exhibit any toxicity to the HeLa cells after exposure with different amounts of NPs.

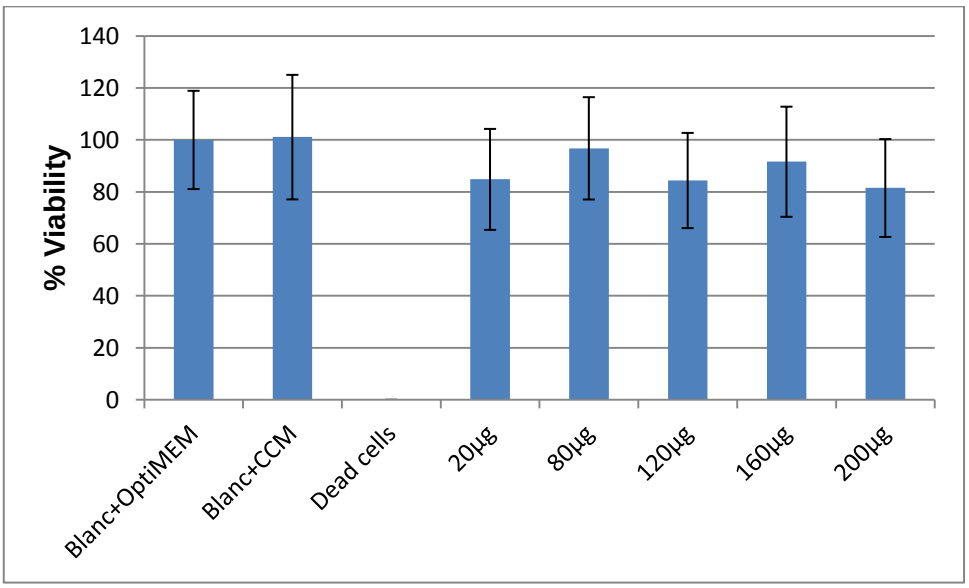

Figure 13. Percentage of viability of HeLa cells after exposure to PLGA Chitosan NPs

3.4.3 Cytotoxicity of protamine coated PLGA NPs

The viability of protamine coated cationic PLGA NPs shows toxicity towards HeLa cells. This result was unexpected since it has already been reported that low concentration of protamine does not show any kind of toxicity (82).

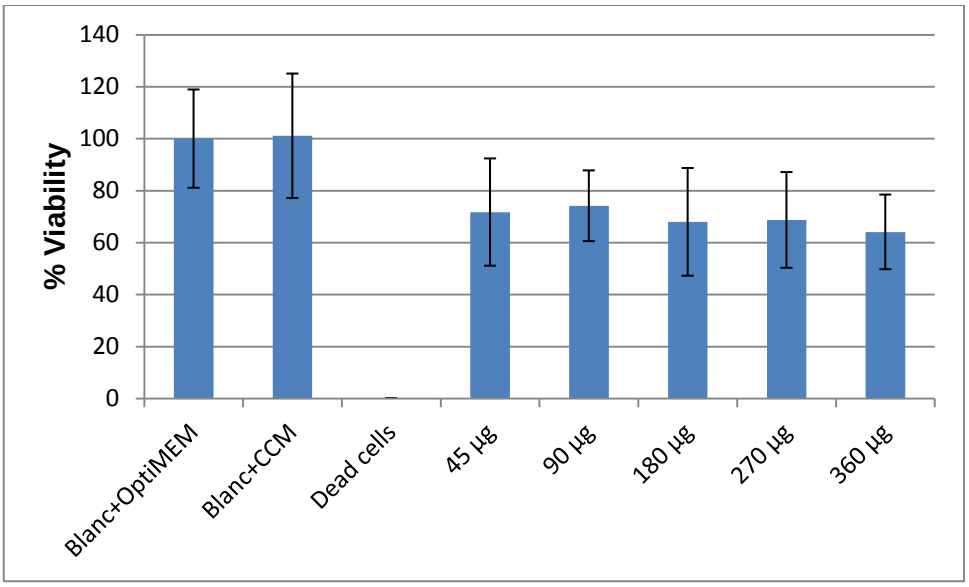

Figure 14. Percentage of viability of HeLa cells after exposure to PLGA Protamine NPs

3.5 Transfection efficiency of cationic PLGA NPs

Flow cytometry is a technique which by the use of hydrodynamic focusing creates a stream of single cells. The cells pass through a laser beam and light is scattered in forward and sideward direction, exciting fluorophores that emit light which is filtered and detected. The fluorescence in this experiment comes from the green fluorescence protein (GFP) encoded by the pDNA used. A cell that gives a green fluorescence signal has undergone transfection. The transfection efficiency is the percentage number of positive fluorescent cells of the total number of cells. The results show the transfection efficiency of the NPs was below 10%.

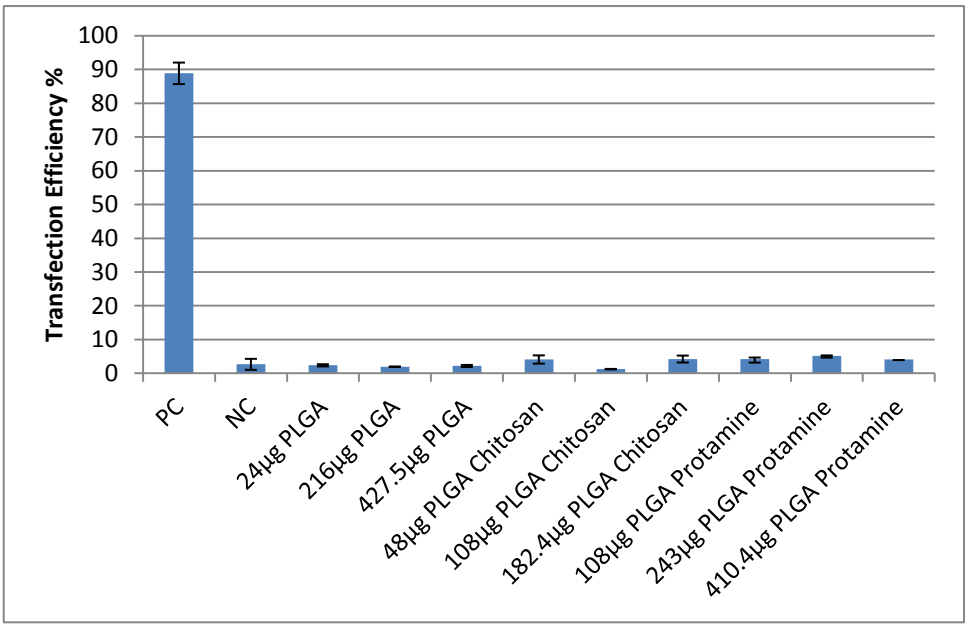

Figure 15. Transfection efficiency of different PLGA NPs

3.6 Fluorescence correlation spectroscopy (FCS) of cationic PLGA NPs

FCS is a microscopy technique that monitors the fluorescence intensity fluctuations of fluorescently labeled molecules which diffuse in and out of the focal volume of a confocal microscope. The free fluorescently labeled alexa647-siRNA molecules are present in the focal volume considered as the reference signal (baseline) and it represents as the initial concentrations of siRNA. Upon complexation of cationic PLGA NPs with alexa647-siRNA, the fluorescence signal decreases with some high fluorescence intensity peak compared to reference signal of initial siRNA. When siRNA releases from the complexes, the concentration of the free alexa647-siRNA increases leading to an increase in the fluorescence signal with decreased peak intensity compared to the signal of the complexes. FCS can be used to quantitatively determine the encapsulation and release of

any fluorescent labeled molecule. In the present study, labeled alexa647-siRNA is complexed with cationic PLGA NPs and their release profile was studied at different time points. It can be observed that the fluorescence intensity decreases when alexa647-siRNA complexes with cationic PLGA NPs shown in Figure 16 and Figure 17. The decreased fluorescence with peak was observed after long incubation time.

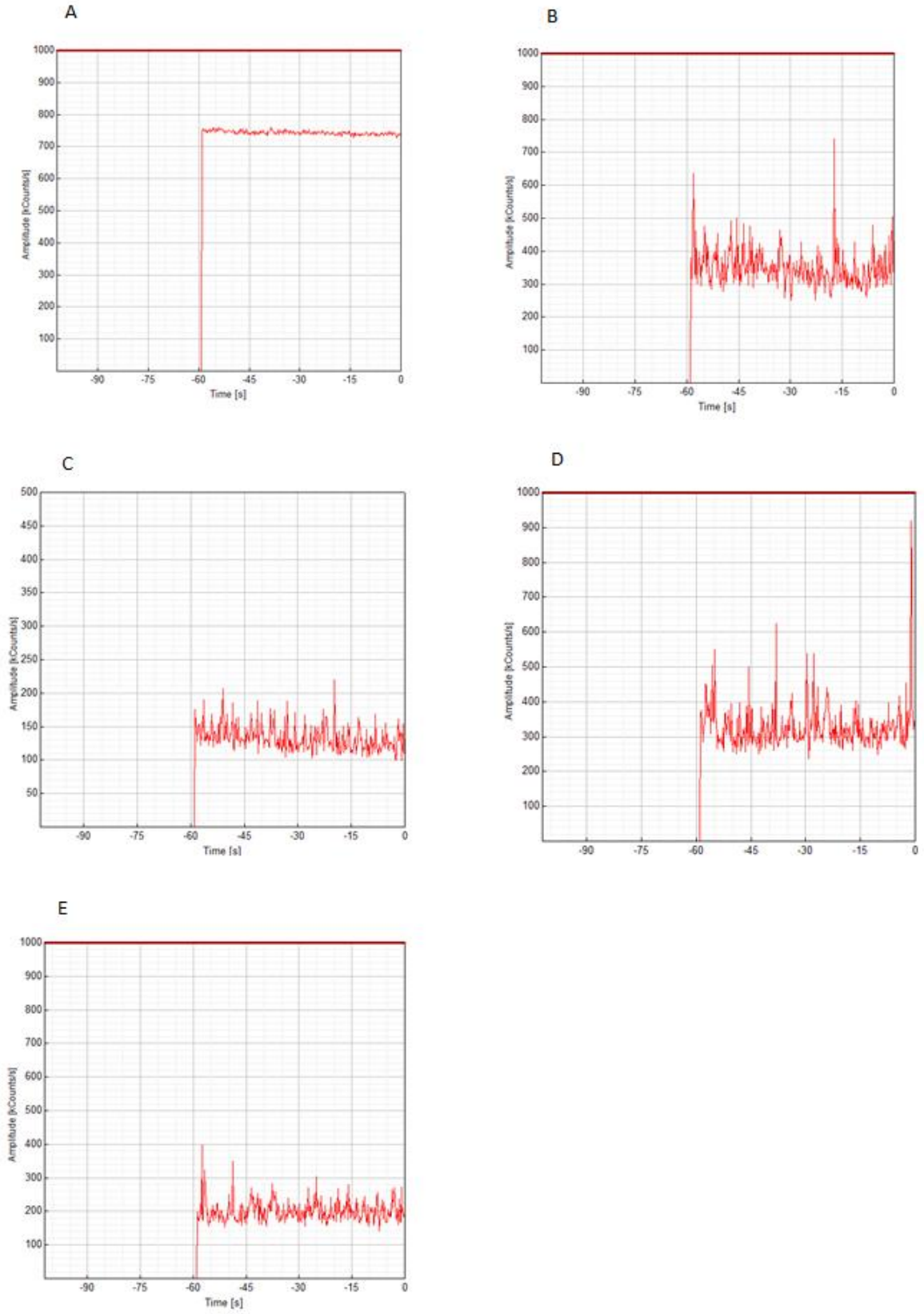

Figure 16. Fluorescence intensity of free labeled siRNA (A); labeled siRNA + PLGA Chitosan (B); labeled siRNA + PLGA Chitosan after 1 h (C); labeled siRNA + PLGA Chitosan after 2 h (D); labeled siRNA + PLGA Chitosan after 24 h (E)

The release of siRNA from the cationic NPs can be controlled by several measurements performed in defined time intervals.

By observing the Figure 17 (A) we can see the condensed siRNA inside the protamine coated PLGA NPs once the fluorescence intensity is lower and the formation of peaks occurred. Figure 17 (B) and (C) show increasing fluorescence intensity probably due to partial libertation of the siRNA from the nanoparticles. Figure 17 (D) shows the diminishing of the fluorescence intensity indicating that the siRNA is probably still encapsulated inside the NPs even after prolonged dispersion in Hepes buffer.

The same experiment was also performed with PLGA Protamine NPs.

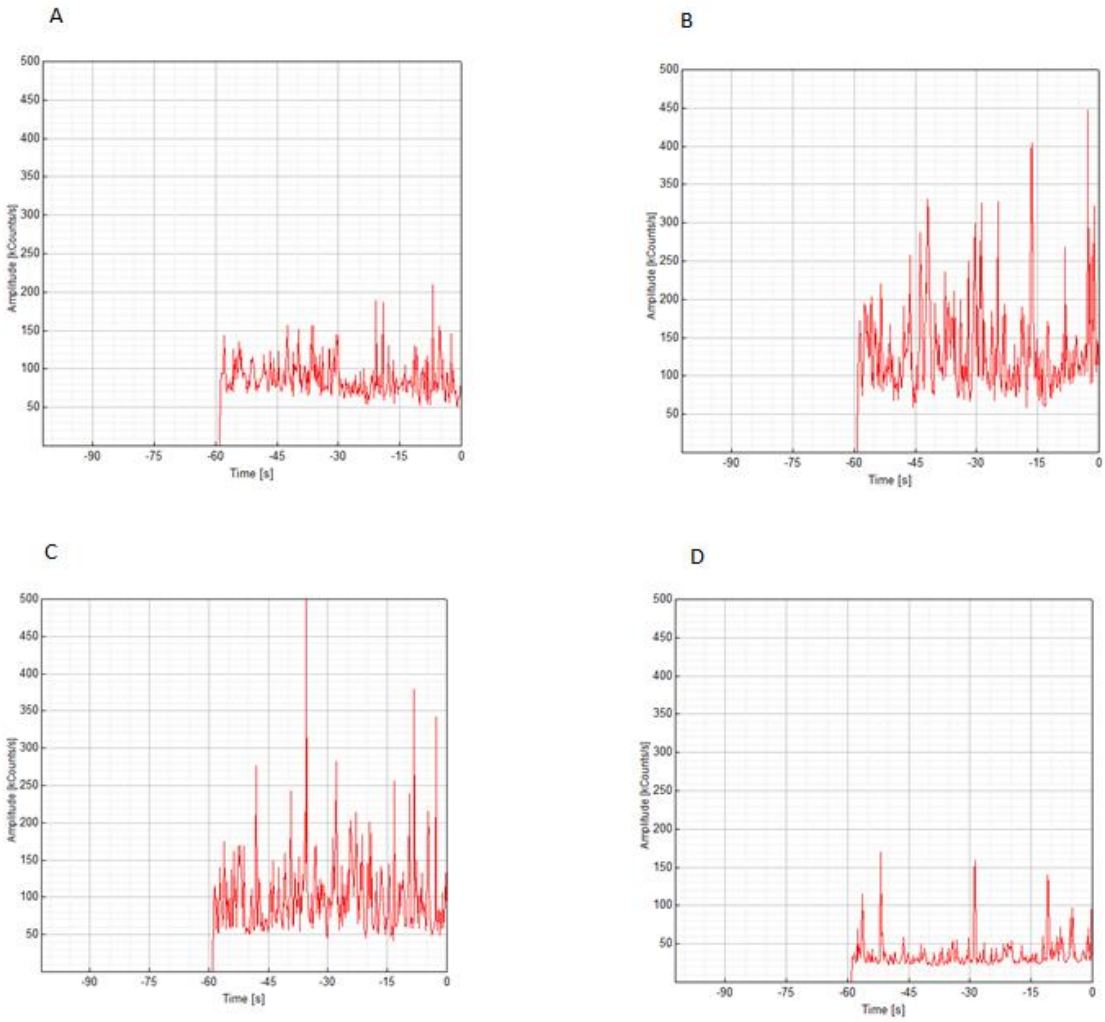

Figure 17. Fluorescence intensity of labeled siRNA + PLGA Protamine NPs (A); labeled siRNA + PLGA Protamine NPs after 1 h (B); labeled siRNA + PLGA Protamine NPs after 2 h (C); labeled siRNA + PLGA Protamine after 24 h (D)

The percentage of release of the siRNA from the nanoparticles observed over time is displayed in Figure 18.

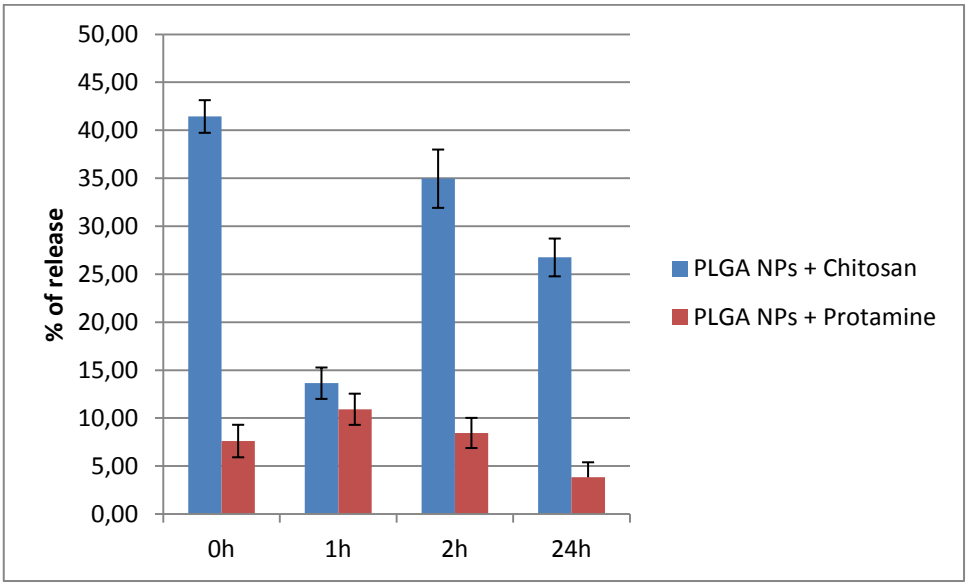

Figure 18. Percentage of release of siRNA over time

The siRNA release kinetics shown in Figure 18 where at time 0h, we can observe the association of siRNA with cationic PLGA NPs. Chitosan coated PLGA NPs shows higher complexation, about 60%, of siRNA, after 24 h it releases to about 14.7%. In case of protamine coated PLGA NPs, shows complexation until 1 h and then release slowly of 3.8% until 24 h of incubation.

3.7 Single Particle Tracking (SPT) of cationic PLGA NPs

SPT tracks the movement of fluorescently labeled NPs and by observing its trajectories in solution it is possible to obtain information about the size of the particles and their interactions with the surroundings. The cationic PLGA NPs complexed with pDNA labeled with GFP were analyzed and their size and movement were assessed. The protamine coated cationic PLGA NPs is shown in Figure 19. It was difficult to analyze chitosan coated PLGA NPs via SPT due to insufficient number of tracks to analyze the trajectories and the right size of the particles.

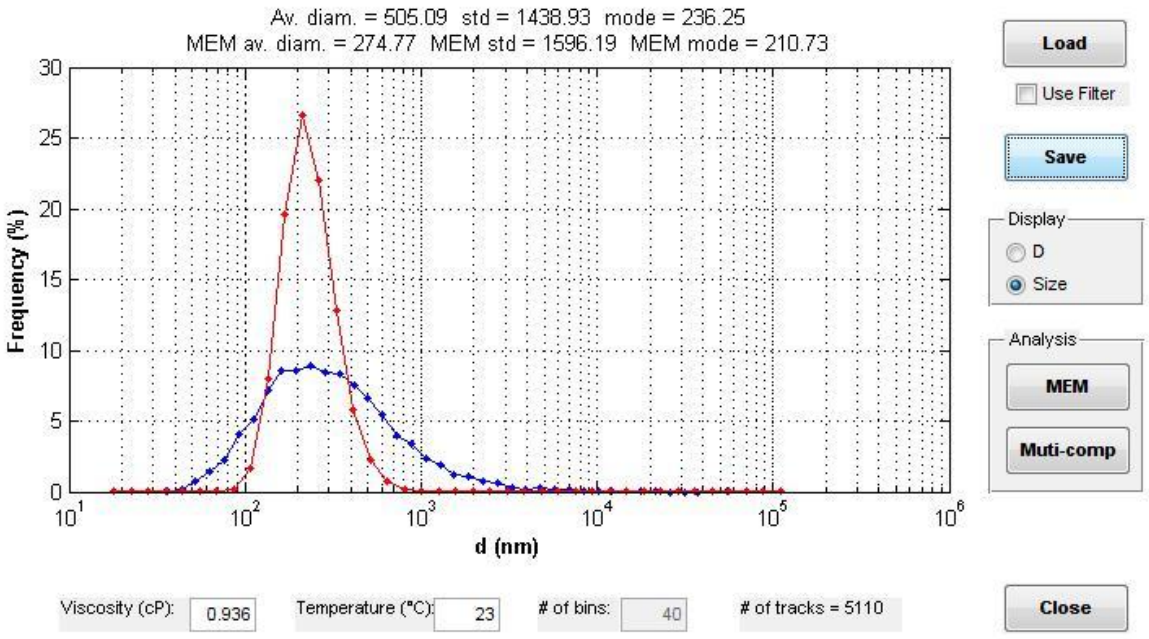

Figure 19. SPT analysis of PLGA + Protamine NPs complexed with pDNA

3.8 Incorporation of Quantum Dots in PLGA NPs

To improve the imaging potential of the prepared NPs, QDs were added to the PLGA solution, to enable its incorporation in the core of the PLGA NPs. The following experiments were performed with these NPs to observe their physic-chemical behavior.

3.8.1 Dinamyc light scattering and UV-Vis measurements

Different concentrations of QDs were evaluated to assess the changes in size, zeta-potential and toxicity of the QDs PLGA NPs.

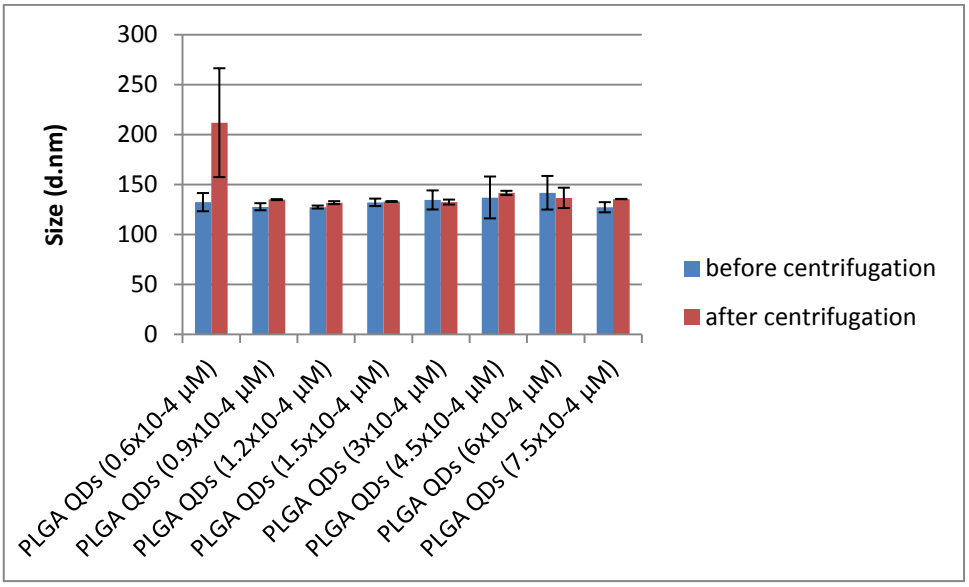

Figure 20. Average size of PLGA QDs NPs

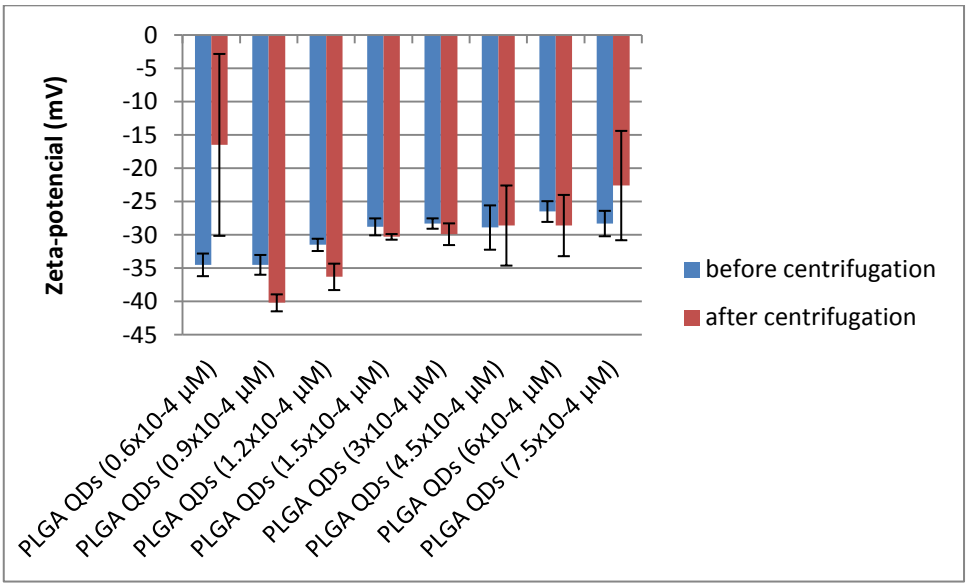

Figure 21. Average zeta-potential of PLGA QDs NPs

Both for size and zeta-potential, no major differences were observed between the different volumes tested.

3.8.1.1 PLGA QDs NPs positively coated with Chitosan or Protamine

The size and surface charge of the PLGA QDs NPs coated with chitosan and protamine are shown in Figure 22 and 23. The results indicate that the higher size and zeta-potential is obtained for the PLGA QDs coated with chitosan (≈ 200 nm; ≈ 60 mV) compared to the one with protamine (≈ 150 nm; ≈ 25 mV). In order to observe the absorbance of the PLGA QDs NPs, UV-Vis measurements were performed but no major difference was observed. The UV-Vis spectrum of PLGA QDs NPs varied with different volumes of QDs as can be

seen in Figure 24. Upon increasing the QDs volume, the absorbance intensity increased and thus imaging properties of the NPs are also expected to be better. However, photoluminescence measurement is needed for better characterization of the PLGA QDs NPs system for imaging applications.

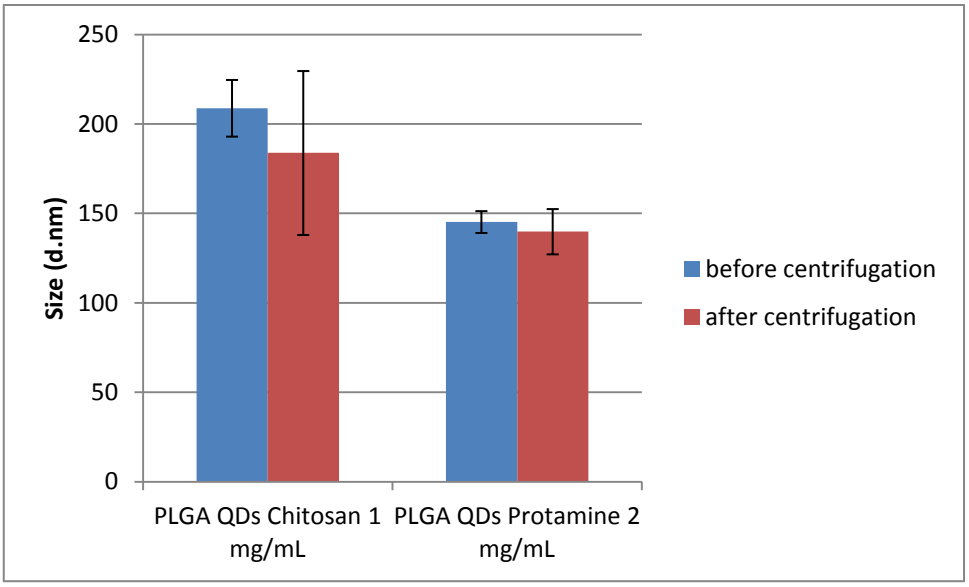

Figure 22. Average size of PLGA QDs NPs positively coated with Chitosan or Protamine

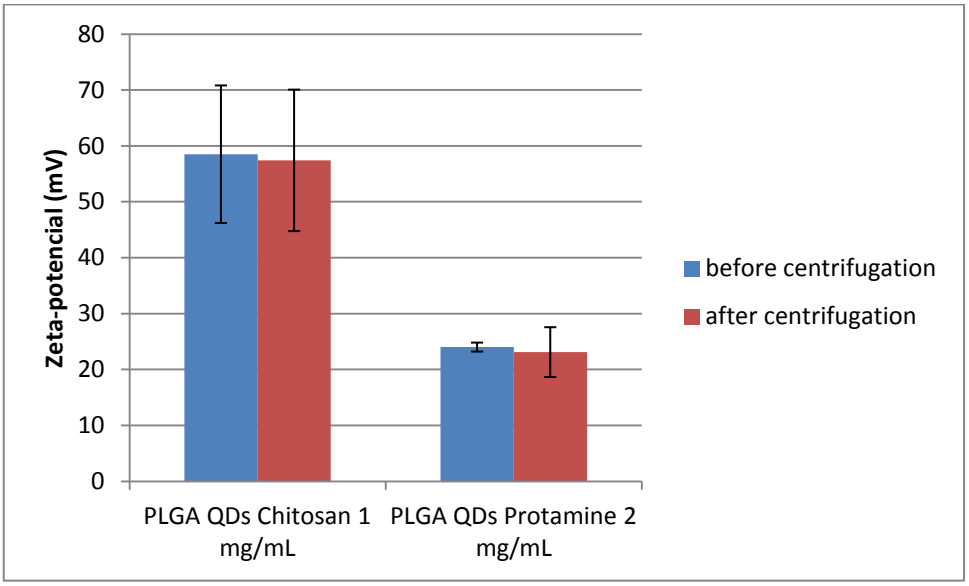

Figure 23. Average Zeta-potencial of PLGA QDs NPs positively coated with Chitosan or Protamine

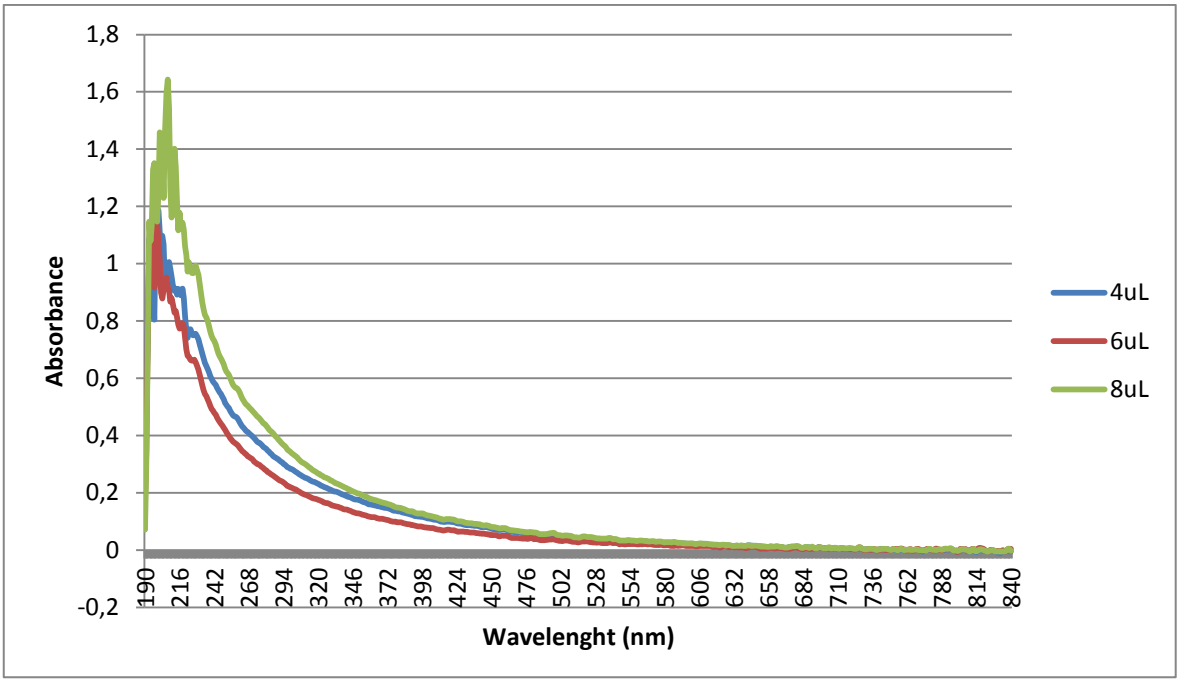

Figure 24. UV-Vis spectrum of PLGA NPs with different volumes of QDs

3.9 Complexation of pDNA with the cationic PLGA QDs NPs

The binding potential of the PLGA QDs NPs with pDNA was assessed by performing the gel electrophoresis and the images were obtained under UV-light.

3.9.1 Chitosan coated PLGA QDs NPs

The result obtained in Figure 25 indicates that chitosan coated PLGA QDs NPs could complex pDNA from 6 µg onwards.

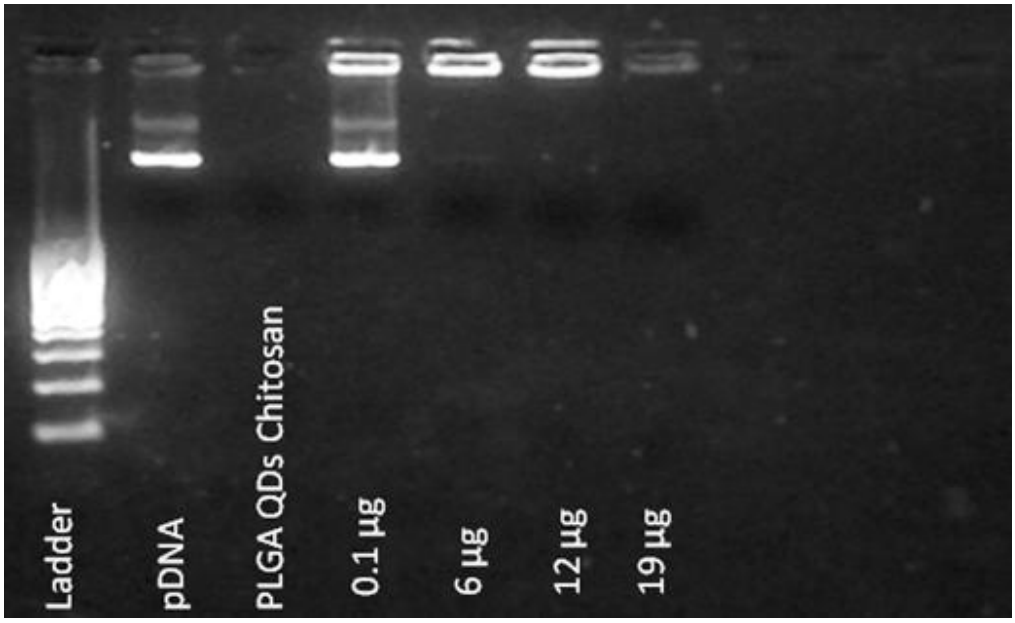

Figure 25. Photo of Gel Electrophoresis of pDNA with PLGA QDs Chitosan NPs

3.9.2 Protamine coated PLGA QDs NPs

In case of protamine coated PLGA QDs NPs, they could complex pDNA from 18 µg onwards as shown in Figure 26. This result is in coherence with zeta-potential result where chitosan coated PLGA QDs NPs show higher positive charge compared to protamine hence complexation with pDNA also starts at lower amount of NPs.

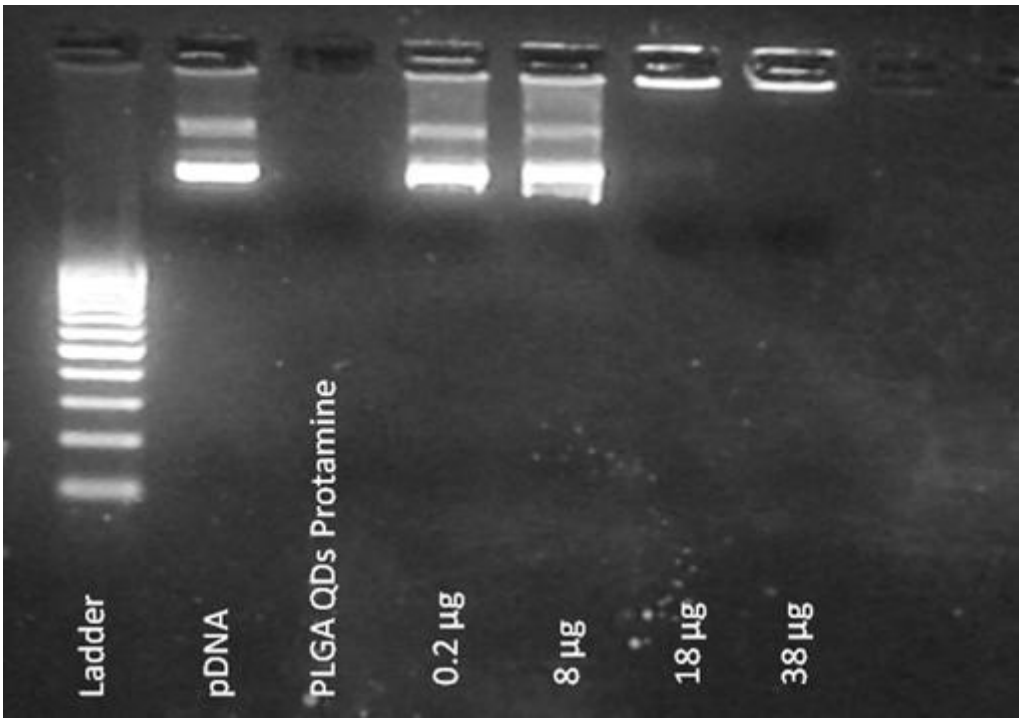

Figure 26. Photo of Gel Electrophoresis of pDNA with PLGA QDs Protamine NPs

3.10 Cytotoxicity of the PLGA QDs NPs

The results of viability of HeLa cells after exposure to PLGA QDs NPs are represented in the Figure 27. It was observed that the PLGA NPs incorporated with up to 7.5×10^{-4} µM of QDs, did not impart cytotoxicity to the cells.

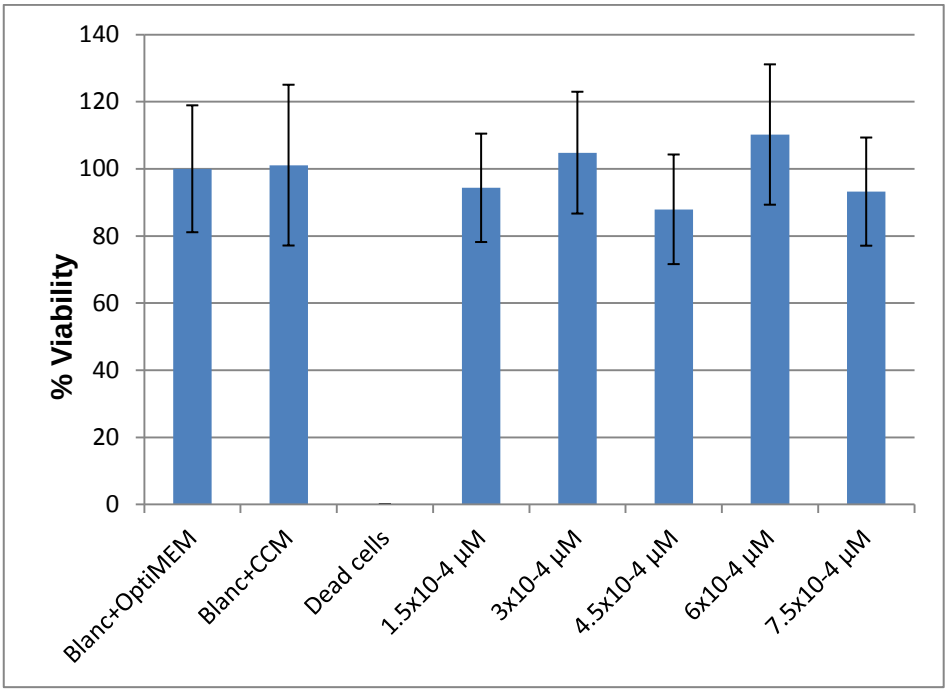

Figure 27. Percentage of viability of HeLa cells after exposure to PLGA QDs NPs

3.11.1 Cytotoxicity of chitosan coated PLGA QDs NPs

The chitosan coated cationic PLGA QDs NPs at different amounts when incubated with HeLa cells showed to provoke a moderate decrease of the viability as compared with controls, although no conclusions can be taken due to the low number of replicates made.

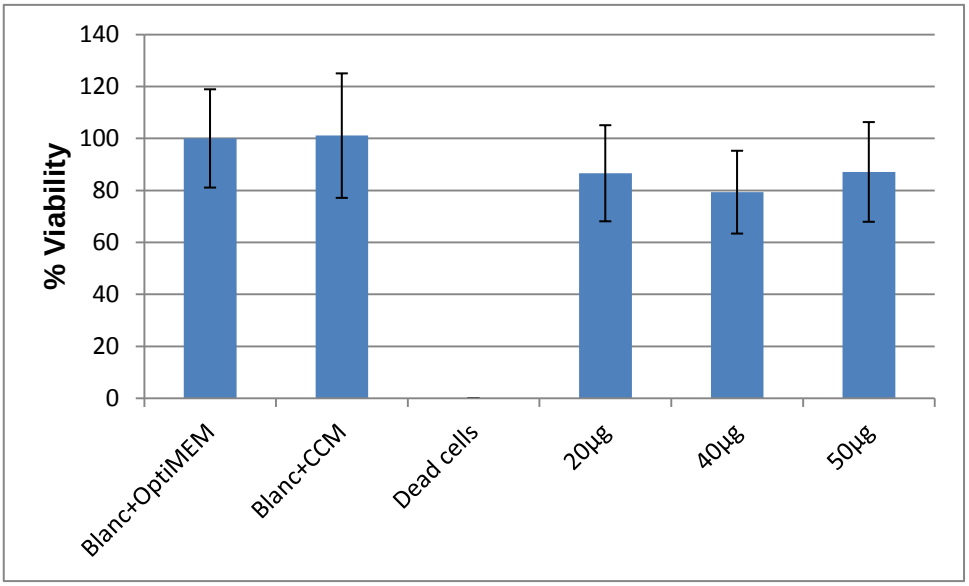

Figure 28. Percentage of viability of HeLa cells after exposure to PLGA QDs Chitosan NPs

3.11.2 Cytotoxicity of protamine coated PLGA QDs NPs

The protamine coated cationic PLGA QDs NPs up to 60 µg did not show toxicity towards HeLa cells.

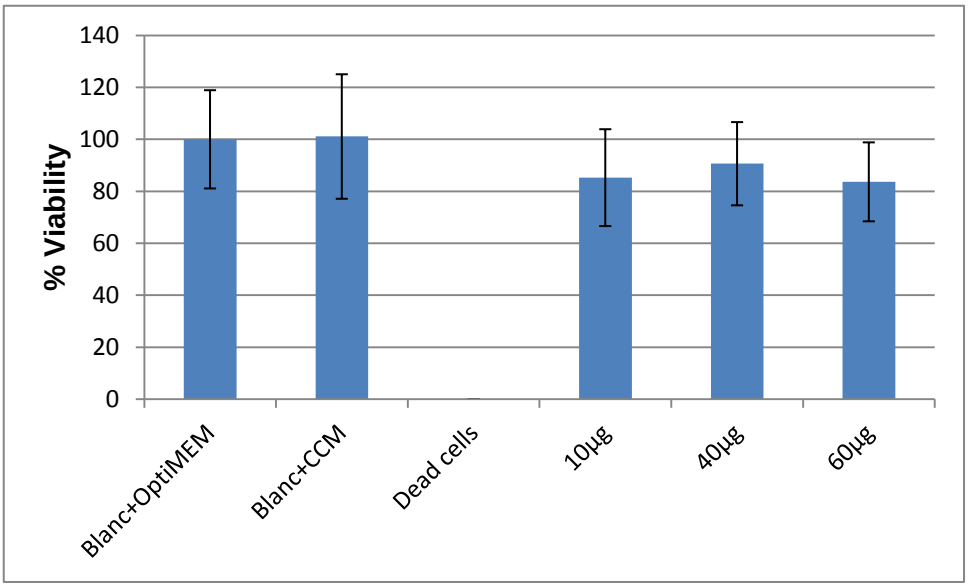

Figure 29. Percentage of viability of PLGA QDs Protamine NPs

4. Discussion

In the present work, the synthesis and characterization of PLGA and gold nanoparticles was performed with different polymeric coatings to obtain particles with cationic charges and imaging properties.

The size variance of the AuNPs was investigated, leading to the conclusion that by varying the concentration of $HAuCl_4$ and reducing/co-reducing agents, different sizes can be achieved. The results obtained show that the most stable AuNPs are the ones prepared at room temperature upon using sodium citrate and sodium borohydride. Polte et al., 2010 studied the differences in the two synthesis methods of AuNPs, by using sodium citrate ("slow" reaction) or $NaBH_4$ ("fast" reaction) (83). Using simultaneously the two reducing agents, we took advantage of the fast reaction provoked by $NaBH_4$ and the monodispersity of the particles offered by sodium citrate, therefore obtaining AuNPs with the best characteristics for our study. Unfortunately, these particles could not be tested for cytotoxicity due to time constraints. Hence, a detailed biological investigation needs to be performed for their potential utilization in therapeutics.

To characterize the PLGA NPs with and without different polymeric coatings, several assays were performed. The size and zeta-potential results on the prepared PLGA NPs indicated that the size of PLGA NPs increases with the increasing concentration of the PLGA solution used in their preparation as already showed by Kara et al, 2014 (87). Cationic polymers chitosan and protamine were used for surface modifications to tentatively enhance biodistribution and pharmacokinetic profile, leading to the increase in size and positive zeta-potential. The chitosan coated PLGA NPs contributed to a higher size, ≈ 200 nm, than protamine coated PLGA NPs, ≈ 150 nm. Baoum et al., 2010 also modified the surface of PLGA NPs with chitosan or protamine and obtained similar sizes for chitosan coating (201 nm). Regarding zeta-potential, they have obtained +36.8 mV with chitosan coating and +17.7 mV with protamine coating, which can be related to the values we obtained, ≈ +40 mV for chitosan coating and ≈ +20 mV for protamine coating. Size of chitosan coating and zeta-potential values are similar to the ones we obtained, specially regarding the difference between the higher zeta-potential conferred by chitosan coating when compared with protamine one (84).

Gel electrophoresis of pDNA complexed with different concentrations of chitosan coated PLGA NPs was performed and it was observed that the NPs from 8 µg onwards show good complexation ability (Figure 10). In case of the protamine coated PLGA NPs, the complete complexation occurs at NPs amount of 18 µg onwards (Figure 11).

The cytotoxicity of the PLGA NPs was assessed using the MTT assay. It was observed that up to 400 µg of PLGA NPs no toxicity was observed towards HeLa cells. When considering chitosan coated cationic PLGA NPs, no toxicity was observed after incubation of the HeLa cells with different amounts of NPs. For protamine coated PLGA NPs the cytotoxicity elicited by these particles was higher than we predicted and the viability of the cells were found to be lower than 70% after 3 hours of incubation with the higher concentrations tested. This result was unexpected since it has already been reported by Arbab et al., that low concentrations of protamine does not show toxicity. In this study, protamine sulfate at concentration up to 50 µg/mL was incubated with different cell types and MTT assay was performed showing no significant loss of viability. The differences seen between both studies can be the concentrations of the solution of protamine used, once our concentration was higher (1 mg/mL) than the maximum tested (50 µg/mL) by Arbab et al. (85).

The transfection efficiency assay was performed to evaluate the effect of the cationic coating, of the NPs complexed with pDNA, on the internalization of the nucleic acid into the cells. The results of this experiment, both regarding PLGA chitosan NPs and PLGA protamine NPs, showed low transfection efficiency, below 10%. It was already reported by Martínez Gómez et al., that protamine coated PLGA microparticles facilitate cell penetration of antigen delivery systems (80). The microparticles used in the study of Martínez Gómez had a much higher size (5.3 µm) than the NPs used in our study (505 nm according to SPT results), as well as zeta-potential (+64.8 mV and +20 mV respectively). These differences can explain the results we obtained once the conclusion reached by Martínez Gómez was that the transfection efficiency was size dependent and only protamine-coated microparticles, which were the biggest, were able to transfect HEK cells.

FCS was performed to see the complexation of the nanoparticles with alexa647-siRNA and the release profiles of siRNA. The association potential was about 60% when considering chitosan coated PLGA NPs and 93 % for protamine coated PLGA NPs. The release rates from both particles after 24 hours were relatively low, showing the high complexation potential between the particles and the siRNA. Jagani et al., 2012 studied the siRNA encapsulation efficiency into chitosan coated PLGA NPs and obtained an association potential of 46.7% and a release rate of the siRNA after 24 hours of approximately 40%. The association potential can be compared to what we have obtained although our release rate was much lower, 14.7%, maybe because the concentrations of PLGA (2 mg/mL) and chitosan (0.4 mg/mL) used by the other authors (86) for the

preparation of the NPs were different from the ones we used, 8mg/mL and 1 mg/mL respectively.

The SPT was made to confirm the nanoparticles size and to see their trajectories and movement in HEPES buffer. The size of the protamine coated PLGA NPs was higher than when measured with DLS but this result is expected due to the complexation of pDNA, which turns the particle into bigger dimensions. The data regarding chitosan coated PLGA NPs was not enough to take conclusions due to the insufficient number of tracks to analyze trajectories and subsequently the nanoparticles' size.

Aiming to improve imaging properties of the nanoparticles prepared, QDs were added to the prepared PLGA solution, incorporating them inside the core of the PLGA NPs, coated either with chitosan or protamine. The size and zeta-potential of these particles was not affected by the addition of QDs, once they have small dimensions (13.4 nm) as compared with the PLGA NPs. The complexation potential of these nanoparticles with pDNA was also assessed. The ability to complex pDNA was observed from 6 µg of NPs coated with chitosan onwards and from 18 µg onwards in case of protamine. Regarding cytotoxicity, the particles didn't show toxicity to HeLa cells up to $7.5x10^{-4}$ µM of QDs used. The chitosan coated PLGA QDs NPs also didn't impart toxicity to cells as well as protamine coated PLGA QDs NPs.

All the assays should be repeated and more toxicity assays should be made to confirm the MTT results, both regarding to positively coated PLGA NPs and PLGA QDs NPs.

5. Conclusions

In the present research a new approach has been adopted for synthesis of inorganic AuNPs and organic biodegradable PLGA NPs.

Monodispersed AuNPs were synthesized at room temperature by simultaneously using two different reducing agents (Sodium citrate and Sodium borohydride) and showed to be more stable and reproducible when compared to those prepared by the conventional method.

The adopted preparation technique of the organic biodegradable PLGA NPs offers better control over size, polydispersity index and surface charge.
The prepared PLGA NPs surface was modified with cationic polymers chitosan or protamine via carbodiimide chemistry, and QDs were incorporated.

The cytotoxicity analysis of the prepared nanocarriers showed no remarkable toxic effects to HeLa cells.

The cationic PLGA NPs showed good nucleic acid complexation ability although did not show good transfection potential.

The utilization of the prepared nanocarriers has to be investigated further in detail.

References

1. Aggarwal P, Hall JB, McLeland CB, Dobrovolskaia MA, McNeil SE. Nanoparticle interaction with plasma proteins as it relates to particle biodistribution, biocompatibility and therapeutic efficacy. Advanced drug delivery reviews. 2009;61(6):428-37.
2. Narayanan D, Geena MG, Lakshmi H, Koyakutty M, Nair S, Menon D. Poly-(ethylene glycol) modified gelatin nanoparticles for sustained delivery of the anti-inflammatory drug Ibuprofen-Sodium: an in vitro and in vivo analysis. Nanomedicine : nanotechnology, biology, and medicine. 2013;9(6):818-28.
3. Bhandari R, Kaur IP. Pharmacokinetics, tissue distribution and relative bioavailability of isoniazid-solid lipid nanoparticles. International journal of pharmaceutics. 2013;441(1-2):202-12.
4. Estanqueiro M, Amaral MH, Conceicao J, Sousa Lobo JM. Nanotechnological carriers for cancer chemotherapy: the state of the art. Colloids and surfaces B: Biointerfaces. 2015;126:631-48.
5. Naahidi S, Jafari M, Edalat F, Raymond K, Khademhosseini A, Chen P. Biocompatibility of engineered nanoparticles for drug delivery. Journal of controlled release : official journal of the Controlled Release Society. 2013;166(2):182-94.
6. Liang XJ, Chen C, Zhao Y, Jia L, Wang PC. Biopharmaceutics and therapeutic potential of engineered nanomaterials. Current drug metabolism. 2008;9(8):697-709.
7. Magdolenova Z, Collins A, Kumar A, Dhawan A, Stone V, Dusinska M. Mechanisms of genotoxicity. A review of in vitro and in vivo studies with engineered nanoparticles. Nanotoxicology. 2014;8(3):233-78.
8. Cole JT, Holland NB. Multifunctional nanoparticles for use in theranostic applications. Drug delivery and translational research. 2015;5(3):295-309.
9. Borel T, Sabliov CM. Nanodelivery of bioactive components for food applications: types of delivery systems, properties, and their effect on ADME profiles and toxicity of nanoparticles. Annual review of food science and technology. 2014;5:197-213.
10. Gratton SE, Ropp PA, Pohlhaus PD, Luft JC, Madden VJ, Napier ME, et al. The effect of particle design on cellular internalization pathways. Proceedings of the National Academy of Sciences of the United States of America. 2008;105(33):11613-8.
11. Wang J, Byrne JD, Napier ME, DeSimone JM. More effective nanomedicines through particle design. Small (Weinheim an der Bergstrasse, Germany). 2011;7(14):1919-31.

12. Laverman P, Boerman OC, Oyen WJ, Dams ET, Storm G, Corstens FH. Liposomes for scintigraphic detection of infection and inflammation. Advanced drug delivery reviews. 1999;37(1-3):225-35.
13. Senior J, Crawley JC, Gregoriadis G. Tissue distribution of liposomes exhibiting long half-lives in the circulation after intravenous injection. Biochimica et biophysica acta. 1985;839(1):1-8.
14. Geng Y, Dalhaimer P, Cai S, Tsai R, Tewari M, Minko T, et al. Shape effects of filaments versus spherical particles in flow and drug delivery. Nature nanotechnology. 2007;2(4):249-55.
15. Doshi N, Prabhakarpandian B, Rea-Ramsey A, Pant K, Sundaram S, Mitragotri S. Flow and adhesion of drug carriers in blood vessels depend on their shape: a study using model synthetic microvascular networks. Journal of controlled release : official journal of the Controlled Release Society. 2010;146(2):196-200.
16. Zhao F, Zhao Y, Liu Y, Chang X, Chen C. Cellular uptake, intracellular trafficking, and cytotoxicity of nanomaterials. Small (Weinheim an der Bergstrasse, Germany). 2011;7(10):1322-37.
17. Wilhelm C, Billotey C, Roger J, Pons JN, Bacri JC, Gazeau F. Intracellular uptake of anionic superparamagnetic nanoparticles as a function of their surface coating. Biomaterials. 2003;24(6):1001-11.
18. Beningo KA, Wang YL. Fc-receptor-mediated phagocytosis is regulated by mechanical properties of the target. Journal of cell science. 2002;115(Pt 4):849-56.
19. Vardharajula S, Ali SZ, Tiwari PM, Eroglu E, Vig K, Dennis VA, et al. Functionalized carbon nanotubes: biomedical applications. International journal of nanomedicine. 2012;7:5361-74.
20. De Jong WH, Borm PJ. Drug delivery and nanoparticles:applications and hazards. International journal of nanomedicine. 2008;3(2):133-49.
21. Saito N, Usui Y, Aoki K, Narita N, Shimizu M, Hara K, et al. Carbon nanotubes: biomaterial applications. Chemical Society reviews. 2009;38(7):1897-903.
22. Zhang W, Guo Z, Huang D, Liu Z, Guo X, Zhong H. Synergistic effect of chemo-photothermal therapy using PEGylated graphene oxide. Biomaterials. 2011;32(33):8555-61.
23. Chang Y, Yang ST, Liu JH, Dong E, Wang Y, Cao A, et al. In vitro toxicity evaluation of graphene oxide on A549 cells. Toxicology letters. 2011;200(3):201-10.
24. Astruc D, Boisselier E, Ornelas C. Dendrimers designed for functions: from physical, photophysical, and supramolecular properties to applications in sensing,

catalysis, molecular electronics, photonics, and nanomedicine. Chemical reviews. 2010;110(4):1857-959.

25. Goldberg M, Langer R, Jia X. Nanostructured materials for applications in drug delivery and tissue engineering. Journal of biomaterials science Polymer edition. 2007;18(3):241-68.

26. Duncan R, Izzo L. Dendrimer biocompatibility and toxicity. Advanced drug delivery reviews. 2005;57(15):2215-37.

27. Boas U, Heegaard PM. Dendrimers in drug research. Chemical Society reviews. 2004;33(1):43-63.

28. Noble GT, Stefanick JF, Ashley JD, Kiziltepe T, Bilgicer B. Ligand-targeted liposome design: challenges and fundamental considerations. Trends in biotechnology. 2014;32(1):32-45.

29. Nakanishi T, Kunisawa J, Hayashi A, Tsutsumi Y, Kubo K, Nakagawa S, et al. Positively charged liposome functions as an efficient immunoadjuvant in inducing cell-mediated immune response to soluble proteins. Journal of controlled release : official journal of the Controlled Release Society. 1999;61(1-2):233-40.

30. Almeida AJ, Souto E. Solid lipid nanoparticles as a drug delivery system for peptides and proteins. Advanced drug delivery reviews. 2007;59(6):478-90.

31. Muller RH, Mader K, Gohla S. Solid lipid nanoparticles (SLN) for controlled drug delivery - a review of the state of the art. European journal of pharmaceutics and biopharmaceutics : official journal of Arbeitsgemeinschaft fur Pharmazeutische Verfahrenstechnik eV. 2000;50(1):161-77.

32. Pardeike J, Hommoss A, Muller RH. Lipid nanoparticles (SLN, NLC) in cosmetic and pharmaceutical dermal products. International journal of pharmaceutics. 2009;366(1-2):170-84.

33. Qiu LY, Bae YH. Polymer architecture and drug delivery. Pharmaceutical research. 2006;23(1):1-30.

34. Li X, Yang Z, Yang K, Zhou Y, Chen X, Zhang Y, et al. Self-assembled polymeric micellar nanoparticles as nanocarriers for poorly soluble anticancer drug ethaselen. Nanoscale research letters. 2009;4(12):1502-11.

35. Pinto Reis C, Neufeld RJ, Ribeiro AJ, Veiga F. Nanoencapsulation I. Methods for preparation of drug-loaded polymeric nanoparticles. Nanomedicine : nanotechnology, biology, and medicine. 2006;2(1):8-21.

36. Xing J, Zhang D, Tan T. Studies on the oridonin-loaded poly(D,L-lactic acid) nanoparticles in vitro and in vivo. International journal of biological macromolecules. 2007;40(2):153-8.

37. Wang S, Zhong Z, Wan J, Tan W, Wu G, Chen M, et al. Oridonin induces apoptosis, inhibits migration and invasion on highly-metastatic human breast cancer cells. The American journal of Chinese medicine. 2013;41(1):177-96.
38. Shenoy DB, Amiji MM. Poly(ethylene oxide)-modified poly(epsilon-caprolactone) nanoparticles for targeted delivery of tamoxifen in breast cancer. International journal of pharmaceutics. 2005;293(1-2):261-70.
39. Kim SY, Lee YM. Taxol-loaded block copolymer nanospheres composed of methoxy poly(ethylene glycol) and poly(epsilon-caprolactone) as novel anticancer drug carriers. Biomaterials. 2001;22(13):1697-704.
40. Kumari A, Yadav SK, Yadav SC. Biodegradable polymeric nanoparticles based drug delivery systems. Colloids and surfaces B, Biointerfaces. 2010;75(1):1-18.
41. De Campos AM, Sanchez A, Alonso MJ. Chitosan nanoparticles: a new vehicle for the improvement of the delivery of drugs to the ocular surface. Application to cyclosporin A. International journal of pharmaceutics. 2001;224(1-2):159-68.
42. Ma P, Mumper RJ. Paclitaxel Nano-Delivery Systems: A Comprehensive Review. Journal of nanomedicine & nanotechnology. 2013;4(2):1000164.
43. Danhier F, Ansorena E, Silva JM, Coco R, Le Breton A, Preat V. PLGA-based nanoparticles: an overview of biomedical applications. Journal of controlled release : official journal of the Controlled Release Society. 2012;161(2):505-22.
44. Fessi H, Puisieux F, Devissaguet JP, Ammoury N, Benita S. Nanocapsule formation by interfacial polymer deposition following solvent displacement. International journal of pharmaceutics. 1989;55(1):R1-R4.
45. Hans ML, Lowman AM. Biodegradable nanoparticles for drug delivery and targeting. Current Opinion in Solid State and Materials Science. 2002;6(4):319-27.
46. Gaumet M, Vargas A, Gurny R, Delie F. Nanoparticles for drug delivery: the need for precision in reporting particle size parameters. European journal of pharmaceutics and biopharmaceutics : official journal of Arbeitsgemeinschaft fur Pharmazeutische Verfahrenstechnik eV. 2008;69(1):1-9.
47. Fonseca C, Simoes S, Gaspar R. Paclitaxel-loaded PLGA nanoparticles: preparation, physicochemical characterization and in vitro anti-tumoral activity. Journal of controlled release : official journal of the Controlled Release Society. 2002;83(2):273-86.
48. Derakhshandeh K, Erfan M, Dadashzadeh S. Encapsulation of 9-nitrocamptothecin, a novel anticancer drug, in biodegradable nanoparticles: factorial design, characterization and release kinetics. European journal of pharmaceutics and biopharmaceutics : official journal of Arbeitsgemeinschaft fur Pharmazeutische Verfahrenstechnik eV. 2007;66(1):34-41.

49. Avgoustakis K, Beletsi A, Panagi Z, Klepetsanis P, Karydas AG, Ithakissios DS. PLGA-mPEG nanoparticles of cisplatin: in vitro nanoparticle degradation, in vitro drug release and in vivo drug residence in blood properties. Journal of controlled release : official journal of the Controlled Release Society. 2002;79(1-3):123-35.
50. Budhian A, Siegel SJ, Winey KI. Production of haloperidol-loaded PLGA nanoparticles for extended controlled drug release of haloperidol. Journal of microencapsulation. 2005;22(7):773-85.
51. Mittal G, Sahana DK, Bhardwaj V, Ravi Kumar MN. Estradiol loaded PLGA nanoparticles for oral administration: effect of polymer molecular weight and copolymer composition on release behavior in vitro and in vivo. Journal of controlled release : official journal of the Controlled Release Society. 2007;119(1):77-85.
52. Cleland JL, Powell MF, Shire SJ. The development of stable protein formulations: a close look at protein aggregation, deamidation, and oxidation. Critical reviews in therapeutic drug carrier systems. 1993;10(4):307-77.
53. Zhu G, Mallery SR, Schwendeman SP. Stabilization of proteins encapsulated in injectable poly (lactide- co-glycolide). Nature biotechnology. 2000;18(1):52-7.
54. Kumar PS, Saini TR, Chandrasekar D, Yellepeddi VK, Ramakrishna S, Diwan PV. Novel approach for delivery of insulin loaded poly(lactide-co-glycolide) nanoparticles using a combination of stabilizers. Drug delivery. 2007;14(8):517-23.
55. Ribeiro S, Hussain N, Florence AT. Release of DNA from dendriplexes encapsulated in PLGA nanoparticles. International journal of pharmaceutics. 2005;298(2):354-60.
56. Kim IS, Lee SK, Park YM, Lee YB, Shin SC, Lee KC, et al. Physicochemical characterization of poly(L-lactic acid) and poly(D,L-lactide-co-glycolide) nanoparticles with polyethylenimine as gene delivery carrier. International journal of pharmaceutics. 2005;298(1):255-62.
57. Patil YB, Swaminathan SK, Sadhukha T, Ma L, Panyam J. The use of nanoparticle-mediated targeted gene silencing and drug delivery to overcome tumor drug resistance. Biomaterials. 2010;31(2):358-65.
58. Tahara K, Sakai T, Yamamoto H, Takeuchi H, Kawashima Y. Establishing chitosan coated PLGA nanosphere platform loaded with wide variety of nucleic acid by complexation with cationic compound for gene delivery. International journal of pharmaceutics. 2008;354(1-2):210-6.
59. Sharma H, Mishra PK, Talegaonkar S, Vaidya B. Metal nanoparticles: a theranostic nanotool against cancer. Drug discovery today. 2015.

60. Rasmussen JW, Martinez E, Louka P, Wingett DG. Zinc oxide nanoparticles for selective destruction of tumor cells and potential for drug delivery applications. Expert opinion on drug delivery. 2010;7(9):1063-77.
61. Kleibert A, Rosellen W, Getzlaff M, Bansmann J. Structure, morphology, and magnetic properties of Fe nanoparticles deposited onto single-crystalline surfaces. Beilstein journal of nanotechnology. 2011;2:47-56.
62. Muddineti OS, Ghosh B, Biswas S. Current trends in using polymer coated gold nanoparticles for cancer therapy. International journal of pharmaceutics. 2015;484(1-2):252-67.
63. Turkevich J, Stevenson PC, Hillier J. A study of the nucleation and growth processes in the synthesis of colloidal gold. Discussions of the Faraday Society. 1951;11(0):55-75.
64. Perrault SD, Chan WC. Synthesis and surface modification of highly monodispersed, spherical gold nanoparticles of 50-200 nm. Journal of the American Chemical Society. 2009;131(47):17042-3.
65. Sakai T, Alexandridis P. Mechanism of gold metal ion reduction, nanoparticle growth and size control in aqueous amphiphilic block copolymer solutions at ambient conditions. The journal of physical chemistry B. 2005;109(16):7766-77.
66. Brust M, Walker M, Bethell D, Schiffrin DJ, Whyman R. Synthesis of thiol-derivatised gold nanoparticles in a two-phase Liquid-Liquid system. Journal of the Chemical Society, Chemical Communications. 1994(7):801-2.
67. Iyer AK, Khaled G, Fang J, Maeda H. Exploiting the enhanced permeability and retention effect for tumor targeting. Drug discovery today. 2006;11(17-18):812-8.
68. Weissleder R. A clearer vision for in vivo imaging. Nature biotechnology. 2001;19(4):316-7.
69. Austin LA, Mackey MA, Dreaden EC, El-Sayed MA. The optical, photothermal, and facile surface chemical properties of gold and silver nanoparticles in biodiagnostics, therapy, and drug delivery. Archives of toxicology. 2014;88(7):1391-417.
70. Rosi NL, Giljohann DA, Thaxton CS, Lytton-Jean AK, Han MS, Mirkin CA. Oligonucleotide-modified gold nanoparticles for intracellular gene regulation. Science (New York, NY). 2006;312(5776):1027-30.
71. Cheng Z, Al Zaki A, Hui JZ, Muzykantov VR, Tsourkas A. Multifunctional nanoparticles: cost versus benefit of adding targeting and imaging capabilities. Science (New York, NY). 2012;338(6109):903-10.
72. Chen F, Ehlerding EB, Cai W. Theranostic nanoparticles. J Nucl Med. 2014;55(12):1919-22.

73. Jordan A, Scholz R, Maier-Hauff K, van Landeghem FK, Waldoefner N, Teichgraeber U, et al. The effect of thermotherapy using magnetic nanoparticles on rat malignant glioma. Journal of neuro-oncology. 2006;78(1):7-14.
74. Huang P, Bao L, Zhang C, Lin J, Luo T, Yang D, et al. Folic acid-conjugated silica-modified gold nanorods for X-ray/CT imaging-guided dual-mode radiation and photo-thermal therapy. Biomaterials. 2011;32(36):9796-809.
75. Mura S, Nicolas J, Couvreur P. Stimuli-responsive nanocarriers for drug delivery. Nature materials. 2013;12(11):991-1003.
76. Staros JV, Wright RW, Swingle DM. Enhancement by N-hydroxysulfosuccinimide of water-soluble carbodiimide-mediated coupling reactions. Analytical biochemistry. 1986;156(1):220-2.
77. Cirillo M, Aubert T, Gomes R, Van Deun R, Emplit P, Biermann A, et al. “Flash” Synthesis of CdSe/CdS Core–Shell Quantum Dots. Chemistry of Materials. 2014;26(2):1154-60.
78. Lucey BP, Nelson-Rees WA, Hutchins GM. Henrietta Lacks, HeLa cells, and cell culture contamination. Archives of pathology & laboratory medicine. 2009;133(9):1463-7.
79. Riss TL, Moravec RA, Niles AL, Benink HA, Worzella TJ, Minor L, et al. Cell Viability Assays. In: Sittampalam GS, Coussens NP, Nelson H, Arkin M, Auld D, Austin C, et al., editors. Assay Guidance Manual. Bethesda MD2004.
80. Martinez Gomez JM, Csaba N, Fischer S, Sichelstiel A, Kundig TM, Gander B, et al. Surface coating of PLGA microparticles with protamine enhances their immunological performance through facilitated phagocytosis. Journal of controlled release : official journal of the Controlled Release Society. 2008;130(2):161-7.
81. Wei X, Zhang Z, Qian Z. Pharmacokinetics and in vivo fate of drug loaded chitosan nanoparticles. Current drug metabolism. 2012;13(4):364-71.
82. Delgado D, del Pozo-Rodriguez A, Solinis MA, Rodriguez-Gascon A. Understanding the mechanism of protamine in solid lipid nanoparticle-based lipofection: the importance of the entry pathway. European journal of pharmaceutics and biopharmaceutics : official journal of Arbeitsgemeinschaft fur Pharmazeutische Verfahrenstechnik eV. 2011;79(3):495-502.
83. Polte Jr, Ralph K, Martin R, Uwe R, Heinrich R, Andreas FT, et al. New insights of the nucleation and growth process of gold nanoparticles via in situ coupling of SAXS and XANES. Journal of Physics: Conference Series. 2010;247(1):012051.
84. Baoum A, Dhillon N, Buch S, Berkland C. Cationic Surface Modification of PLG Nanoparticles Offers Sustained Gene Delivery to Pulmonary Epithelial Cells. Journal of pharmaceutical sciences. 2010;99(5):2413-22.

85. Arbab AS, Yocum GT, Kalish H, Jordan EK, Anderson SA, Khakoo AY, et al. Efficient magnetic cell labeling with protamine sulfate complexed to ferumoxides for cellular MRI. Blood. 2004;104(4):1217-23.

86. Jagani HV, Josyula VR, Palanimuthu VR, Hariharapura RC, Gang SS. Improvement of therapeutic efficacy of PLGA nanoformulation of siRNA targeting anti-apoptotic Bcl-2 through chitosan coating. European Journal of Pharmaceutical Sciences. 2013;48(4–5):611-8.

87 Kara A, Ozturk N, Sarisozen C, Vural I. Investigation of formulation parameters of PLGA nanoparticles prepared by nanoprecipitation technique. Proceedings of the 5th Internacional conference on Nanothechnology: Fundamentals and Applications, Czech Republic. Prague; 2014.

Supplement 1

Table 4 DLS measurements of AuNPs formed using Sodium citrate in different concentrations and temperatures

Composition	Size (d.nm)	PDI	Temperature conditions
1mL $HAuCl_4$ + 1mL H_2O + 500µL Sodium citrate	177.1	0.225	Room temperature
1mL $HAuCl_4$ + 1mL H_2O + 1mL Sodium citrate	26.89	0.572	Room temperature
1mL $HAuCl_4$ + 1mL H_2O + 500µL Sodium citrate	58.41	0.273	90°C
1mL $HAuCl_4$ + 1mL H_2O + 1mL Sodium citrate	24.08	0.348	90°C
2mL $HAuCl_4$ + 2mL Sodium citrate	225.6	0.371	90°C
2mL $HAuCl_4$ + 5mL Sodium citrate	14.57	0.570	90°C
2mL $HAuCl_4$ + 2mL H_2O + 1mL Sodium citrate	95.65	0.182	90°C
2mL $HAuCl_4$ + 2mL H_2O + 2mL Sodium citrate	17.86	0.611	Room temperature
1mL $HAuCl_4$ + 1mL H_2O + 500µL Sodium citrate	65.34	0.270	90°C

1mL $HAuCl_4$ + 1mL H_2O + 1mL Sodium citrate	20.11	0.626	90°C
1mL $HAuCl_4$ + 1mL H_2O + 500µL Sodium citrate	131.6	0.091	Room temperature
1mL $HAuCl_4$ + 1mL H_2O + 1mL Sodium citrate	40.06	0.434	Room temperature

Table 5 DLS measurements of AuNPs formed using Sodium citrate and $NaBH_4$ in different concentrations and temperatures

Composition	Size (d.nm)	PDI	Temperature conditions
2mL $HAuCl_4$ + 2mL Sodium citrate + 1mL $NaBH_4$	48.53	0.234	90°C
2mL $HAuCl_4$ + 2mL Sodium citrate + 1mL $NaBH_4$	20.15	0.647	0°C
2mL $HAuCl_4$ + 2mL Sodium citrate + 1mL $NaBH_4$	29.64	0.349	Room temperature
2mL $HAuCl_4$ + 2mL Sodium citrate + 500µL $NaBH_4$	37.95	0.904	Room temperature
2mL $HAuCl_4$ + 2mL Sodium citrate + 500µL $NaBH_4$	43.875	0.672	0°C
2mL $HAuCl_4$ + 2mL Sodium citrate + 300µL $NaBH_4$	57.09	0.655	90°C

2mL $HAuCl_4$ + 2mL Sodium citrate + 500µL $NaBH_4$	20.99	0.658	90°C
2mL $HAuCl_4$ + 1mL Sodium citrate + 500µL $NaBH_4$	63.96	0.648	90°C
2mL $HAuCl_4$ + 2mL Sodium citrate + 1mL $NaBH_4$	23.1	0.684	90°C
2mL $HAuCl_4$ + 2mL Sodium citrate + 1mL $NaBH_4$	42.89	1	90°C
1mL $HAuCl_4$ + 1mL H_2O + 500µL Sodium citrate + 200µL $NaBH_4$	20.9	0.272	Room temperature
1mL $HAuCl_4$ + 1mL H_2O + 1mL Sodium citrate + 100µL $NaBH_4$	17.19	0.293	Room temperature
1mL $HAuCl_4$ + 1mL H_2O + 1mL Sodium citrate + 50µL $NaBH_4$	30.76	0.215	Room temperature
1mL $HAuCl_4$ + 1mL H_2O + 1mL Sodium citrate + 50µL $NaBH_4$	22.02	0.338	90°C
1mL $HAuCl_4$ + 1mL H_2O + 500µL Sodium citrate + 200µL $NaBH_4$	38.62	0.196	Room temperature
1mL $HAuCl_4$ + 1mL H_2O + 500µL Sodium citrate + 200µL $NaBH_4$	69.57	0.149	90°C
1mL $HAuCl_4$ + 1mL H_2O + 1mL Sodium citrate + 100µL $NaBH_4$	28.59	0.100	Room temperature
1mL $HAuCl_4$ + 1mL H_2O + 1mL Sodium citrate +	22.50	0.183	90°C

100µL $NaBH_4$			
1mL $HAuCl_4$ + 1mL H_2O + 1mL Sodium citrate + 50µL $NaBH_4$	41.66	0.094	Room temperature
1mL $HAuCl_4$ + 1mL H_2O + 1mL Sodium citrate + 50µL $NaBH_4$	142.4	0.283	90°C
1mL $HAuCl_4$ + 1mL H_2O + 500µL Sodium citrate + 200µL $NaBH_4$	29.58	0.203	Room temperature
1mL $HAuCl_4$ + 1mL H_2O + 500µL Sodium citrate + 200µL $NaBH_4$	19.09	0.438	90°C
1mL $HAuCl_4$ + 1mL H_2O + 1mL Sodium citrate + 100µL $NaBH_4$	158.7	0.253	Room temperature
1mL $HAuCl_4$ + 1mL H_2O + 1mL Sodium citrate + 100µL $NaBH_4$	64.85	0.138	90°C
1mL $HAuCl_4$ + 1mL H_2O + 1mL Sodium citrate + 50µL $NaBH_4$	18.60	0.258	Room temperature
1mL $HAuCl_4$ + 1mL H_2O + 1mL Sodium citrate + 50µL $NaBH_4$	48.08	0.106	90°C
1mL $HAuCl_4$ + 1mL H_2O + 500µL Sodium citrate + 200µL $NaBH_4$	41.43	0.215	Room temperature
1mL $HAuCl_4$ + 1mL H_2O + 500µL Sodium citrate + 200µL $NaBH_4$	41.08	0.206	Room temperature
1mL $HAuCl_4$ + 1mL H_2O + 1mL Sodium citrate + 100µL $NaBH_4$	16.66	0.199	Room temperature
1mL $HAuCl_4$ + 1mL H_2O +	17.83	0.339	Room

1mL Sodium citrate + 100µL $NaBH_4$			temperature
1mL $HAuCl_4$ + 1mL H_2O + 1mL Sodium citrate + 50µL $NaBH_4$	18.49	0.320	Room temperature
1mL $HAuCl_4$ + 1mL H_2O + 1mL Sodium citrate + 50µL $NaBH_4$	18.12	0.316	Room temperature
1mL $HAuCl_4$ + 500µL Sodium citrate + 200µL $NaBH_4$	41.11	0.198	Room temperature
1mL $HAuCl_4$ + 500µL Sodium citrate + 200µL $NaBH_4$	38.47	0.192	Room temperature
2mL $HAuCl_4$ + 2mL H_2O + 1mL Sodium citrate + 400µL $NaBH_4$	157.8	0.248	Room temperature
2mL $HAuCl_4$ + 2mL H_2O + 2mL Sodium citrate + 200µL $NaBH_4$	53.97	0.275	90°C
2mL $HAuCl_4$ + 2mL H_2O + 2mL Sodium citrate + 100µL $NaBH_4$	23.89	0.508	90°C
1mL $HAuCl_4$ + 1mL H_2O + 500µL Sodium citrate + 200µL $NaBH_4$	94.32	0.158	90°C
1mL $HAuCl_4$ + 1mL H_2O + 1mL Sodium citrate + 100µL $NaBH_4$	54.61	0.577	90°C
1mL $HAuCl_4$ + 1mL H_2O + 1mL Sodium citrate + 50µL $NaBH_4$	17.74	0.280	90°C
1mL $HAuCl_4$ + 1mL H_2O + 500µL Sodium citrate + 200µL $NaBH_4$	28.14	0.404	Room temperature

1mL $HAuCl_4$ + 1mL H_2O + 1mL Sodium citrate + 100µL $NaBH_4$	25.86	0.169	Room temperature
1mL $HAuCl_4$ + 1mL H_2O + 1mL Sodium citrate + 50µL $NaBH_4$	17.61	0.453	Room temperature
1mL $HAuCl_4$ + 1mL H_2O + 1mL Sodium citrate + 200µL $NaBH_4$	33.89	0.269	Room temperature
1mL $HAuCl_4$ + 1mL H_2O + 1mL Sodium citrate + 100µL $NaBH_4$	45.07	0.240	Room temperature

Table 6 DLS measurements of AuNPs formed using $NaBH_4$ in different concentrations and temperatures

Composition	Size (d.nm)	PDI	Temperature conditions
1mL $HAuCl_4$ + 1mL H_2O + 50µL $NaBH_4$	22.94	0.541	Room temperature
1mL $HAuCl_4$ + 1mL H_2O + 200µL $NaBH_4$	482.2	0.551	Room temperature
1mL $HAuCl_4$ + 1mL H_2O + 100µL $NaBH_4$	90.13	0.141	Room temperature
1mL $HAuCl_4$ + 1mL H_2O + 50µL $NaBH_4$	60.74	0.396	Room temperature

Table 7 DLS measurements of AuNPs formed using $NaBH_4$ and CTAB in different concentrations and temperatures

Composition	Size (d.nm)	PDI	Temperature conditions
200µL $HAuCl_4$ + 200µL CTAB	55.27	0.236	90°C
1mL $HAuCl_4$ + 1mL H_2O + 200µL $NaBH_4$ + 500µL CTAB	103.4	0.432	Room temperature
1mL $HAuCl_4$ + 1mL H_2O + 100µL $NaBH_4$ + 1mL CTAB	126.4	0.407	Room temperature
1mL $HAuCl_4$ + 1mL H_2O + 100µL $NaBH_4$ + 1mL CTAB	126.4	0.407	Room temperature
1mL $HAuCl_4$ + 1mL H_2O + 50µL $NaBH_4$ + 1mL CTAB	166.4	0.431	Room temperature

Table 8 DLS measurements of AuNPs formed using bPEI in different concentrations and temperatures

Composition	Size (d.nm)	PDI	Temperature conditions
1mL $HAuCl_4$ + 1mL H_2O + (25µL of bPEI + 75µL H_2O)	790.1	0.717	90°C
1mL $HAuCl_4$ + 1mL H_2O + (25µL bPEI + 75µL H_2O)	1718	1	90°C
2mL $HAuCl_4$ + 100µL bPEI	260.1	0.314	90°C
1mL $HAuCl_4$ + 1mL H_2O + (25µL bPEI + 75µL H_2O)	289.8	0.345	90°C
1mL $HAuCl_4$ + 1mL H_2O + (50µL bPEI + 50µL H_2O)	2002	1	90°C
1mL $HAuCl_4$ + 1mL H_2O + (75µL bPEI + 75µL H_2O)	196	0.377	90°C
1mL $HAuCl_4$ + 1mL H_2O + (25µL bPEI + 75µL H_2O)	42.59	0.118	90°C

Table 9 DLS measurements of AuNPs formed using Oleic acid or Olive oil in different concentrations and temperatures

Composition	Size (d.nm)	PDI	Temperature conditions
1mL $HAuCl_4$ (solution 1mg/mL in acetone) + 100µL Oleic acid	637.1	0.480	Room temperature
1mL $HAuCl_4$ + 1mL H_2O + 2µL Olive oil	291.4	0.415	Room temperature
1mL $HAuCl_4$ + 1mL H_2O + 100µL Olive oil	101.6	0.358	Room temperature

Table 10 DLS measurements of AuNPs formed using $NaBH_4$ and Alginic acid in different concentrations and temperatures

Composition	Size (d.nm)	PDI	Temperature conditions
1mL $HAuCl_4$ + 1mL H_2O + 1mL Alginic acid	242	0.289	90°C
1mL $HAuCl_4$ + 1mL H_2O + 200µL Alginic acid + 600µL $NaBH_4$	41.4	0.265	90°C
1mL $HAuCl_4$ + 1mL H_2O + 250µL Alginic acid + 50µL $NaBH_4$	44.97	0.247	90°C
1mL $HAuCl_4$ + 1mL H_2O + 250µL Alginic acid + 250µL $NaBH_4$	95.03	0.417	90°C
1mL $HAuCl_4$ + 1mL H_2O + 250µL Alginic acid + 500µL $NaBH_4$	79.20	0.495	90°C
1mL $HAuCl_4$ + 1mL H_2O + 2500µL Alginic acid + 1mL $NaBH_4$	26.53	0.556	90°C
1mL $HAuCl_4$ + 1mL H_2O + 250µL Alginic acid + 100µL $NaBH_4$	45.45	0.263	90°C
1mL $HAuCl_4$ + 1mL H_2O + 250µL Alginic acid + 400µL $NaBH_4$	50.17	1	90°C
1mL $HAuCl_4$ + 1mL H_2O + 200µL Alginic acid + 600µL $NaBH_4$	45.95	0.193	90°C
1mL $HAuCl_4$ + 1mL H_2O + 250µL Alginic acid + 50µL $NaBH_4$	39.25	0.373	90°C